Effects of sympathetic modulation by renal denervation on hepatosteatosis and liver RAGE/sRAGE balance

Authors: Simina-Ramona Selejan [1]*†, Dominik Linz [1]†, Mathias Hohl[1], Juliane Dederer[1], Andrey Kazakov[1], Olesia Zamyatkin[1], Lucas Lauder[1], Thimoteus Speer[2], Marcin Krawczyk[3], Frank Lammert[3], Felix Mahfoud[1,] Michael Böhm[1]

† S. Selejan and D. Linz contributed equally to this study

Affiliations:

[1] Department of Internal Medicine III, Cardiology, Angiology and Intensive Care Medicine University of Saarland, Homburg, Germany.

[2] Department of Internal Medicine IV, Nephrology, University of Saarland, Homburg, Germany.

[3] Department of Internal Medicine II, Gastroenterology, Endocrinology and Diabetology, University of Saarland, Homburg, Germany.

* Simina-Ramona Selejan, MD; Klinik für Innere Medizin III, Kirrbergerstr. 100, Geb. 41.1 (IMED); Universität des Saarlandes; D-66421 Homburg/Saar; Phone +49-6841-16-15031; Fax: +49-6841-16-15031. e-mail: simina.selejan@uks.eu

Classification: research article

Key words: metabolic syndrome, fatty liver, renal denervation, Receptor for Advanced Glycation End products

Abstract

The metabolic syndrome (MetS) is associated with increased sympathetic activity and dysbalance of "Receptor-for-Advanced-Glycation-End-products" (RAGE) and its soluble receptor decoy sRAGE, which may be involved in liver tissue remodeling. The effects of sympathetic modulation by renal denervation (RDN) on hepatic remodeling and liver RAGE/sRAGE balance are unknown. In a rat model for MetS, RDN reduced hepatic RAGE expression and increased sRAGE levels, which was accompanied by reduced hepatic steatosis and liver fibrosis. In patients undergoing RDN with documented blood pressure reductions, sRAGE plasma levels were increased and alanine aminotransferase values were reduced 6 months after the procedure. In vitro lipid accumulation and RAGE expression were induced in HepG2 cells by ß-adrenergic receptor stimulation and could be reduced by pretreatment with sRAGE. In conclusion, RDN reduces hepatic steatosis and injury by improving liver RAGE/sRAGE balance. These findings may open new avenues for interventional strategies to treat metabolic liver disease beyond hypertension.

Significance statement

Fatty liver is a risk factor for cirrhosis and hepatocellular carcinoma and a growing problem worldwide. Here we show in rodent and human models of metabolic syndrome, that sympathoadrenergic activity contributes to the development of fatty liver and that inhibition of the sympathetic tone by renal denervation (RDN) is protective. On the cellular level we observed that Receptor for Advanced Glycation End products (RAGE) is regulated via adrenergic stimulation and leads to cellular fat accumulation. RDN already being applied as therapy option for arterial hypertension, prospective clinical trials are warranted to address the effectivity of RDN in the treatment and prevention of fatty liver disease.

Introduction

Nonalcoholic fatty liver disease (NAFLD) is increasingly common in patients with metabolic syndrome (MetS) (**1-2**) and includes pathological conditions ranging from hepatic steatosis, steatohepatitis and fibrosis to cirrhosis and hepatocellular carcinoma (**3-4**). NAFLD is determined by a complex network of metabolic processes resulting in hepatic lipid accumulation, impaired insulin signaling (**5**) and hepatic inflammation (nonalcoholic steatohepatitis, NASH) **(6).** MetS itself is associated with both, increased sympathetic activity (**7-8**) and high levels of advanced glycation end products (AGEs) (**9**), a heterogenous class of non-enzymatic protein glycation adducts binding to their cell-surface receptor for advanced glycation end products (RAGE) and inducing reactive oxygen species generation involved in pro-inflammatory and pro-fibrotic responses (**10-12**). RAGE can be cleaved by metalloproteinases to soluble RAGE (sRAGE), which serves as a protective decoy receptor neutralizing RAGE-ligands and also blocking RAGE itself (**13-15**). Decreased sRAGE plasma concentrations have been described in patients with MetS (**16**) and fatty liver disease (**7, 17**), but the responsible mechanisms are still unclear.

Renal sympathetic denervation (RDN) can reduce renal and central sympathetic activity (**18-19**). RDN has been shown to lower blood pressure and provide beneficial cardiovascular effects in rats with metabolic syndrome (**20-22**) and in patients with resistant hypertension and associated metabolic disorders (**7, 23**). Its effects on hepatic disease in MetS are unknown. In this study, we explored the effects of sympathetic modulation by RDN on hepatic fat accumulation, liver injury and fibrosis, and the link to the RAGE-sRAGE system in a rat model of hypertension, MetS and liver steatosis induced by a leptin receptor mutation. In a translational approach, we investigated these RDN-induced alterations in hypertension patients undergoing RDN.

Results

Rat experiments

Metabolic parameters: Physiological and metabolic parameters are summarized in **Table 1**. In SHRob rats, glomerular filtration rate (GFR) was reduced compared with controls (-68%, p<0.00001), but was significantly increased after RDN (+105% versus SHRob, p=0.0012). Creatinine levels also showed a decrease after RDN (-40% versus SHRob). Fasting insulin levels were significantly increased in SHRob compared with controls (+1358%, p=0.0002) and showed a numerical decrease after RDN without statistical significance (**Table 1**). HbA1c data were similar in all groups (**Table 1**). Cholesterol and triglyceride concentrations were increased in SHRob without significant change after RDN (**Table 1**). Alanine aminotransferase (ALT) activity was significantly increased in SHRob (+77% versus controls, p<0.0001) and was reduced by RDN (-36% versus SHRob, p=0.0003). No significant differences in aspartate aminotransferase (AST) were observed.

Renal denervation and liver norepinephrine concentrations: A reduction in renal norepinephrine tissue content was observed in RDN-treated SHRob rats (SHRobRDN) three months after the procedure compared to sham-operated SHRob indicating successful sympathetic denervation (**Table 1**; 96.9±7.5 in SHRob vs. 6.73±1.9 pg/ml in SHRobRDN, p=0.0009). Similarly, liver norepinephrine content was reduced in SHRobRDN versus SHRob (p=0.007; **Table 2**, **Fig. 1A**) and tyrosine hydroxylase activity, the enzyme catalyzing the rate limiting step in the synthesis of catecholamines, was decreased after RDN, as depicted by the phospho-tyrosine/total tyrosine hydroxylase ratio (-43% versus SHRob, p=0.031; **Table 2**, **Fig. 1B**). Both parameters correlated with renal norepinephrine content (**Fig. 1C-D**; r=0.75, p=0.02 for liver tyrosine hydroxylase activity and r=0.89, p=0.002 for liver norepinephrine versus renal norepinephrine content) and with each other (**Fig. 1E**; r=0.82, p=0.005 for liver tyrosine hydroxylase activity versus liver norepinephrine). On the other hand, renal denervation did not significantly alter liver expression of beta-adrenergic receptors (**Fig. 1F**).

Renal denervation and liver injury: The degree of hepatic steatosis (**Table 2**, **Fig. 2A+2B**) is significantly increased in SHRob (**Table 2**, **Fig. 2B**: +341% versus controls, p=0.0004), and this increase was attenuated by RDN (-59% versus SHRob; p=0.0024). Measurement of adipose differentiation related protein (ADRP) as marker of lipid droplet accumulation confirmed the increase in lipid accumulation in SHRob (**Table 2**, **Fig. 2C**: +285% in SHRob versus Control, p=0.008) and a reduction of ADRP contents after RDN (-58% versus SHRob, p=0.033). Liver pro-apoptotic Bcl-2-associated X protein (BAX) expression, as assessed by immunoblot analysis (**Fig. 2D**, upper panel), was significantly increased in SHRob as compared to normotensive lean controls (**Table 2**, **Fig. 2D**, lower panel: 27fold increase in SHRob versus controls (p<0.0001). BAX expression decreased after RDN (-39% in SHRobRDN versus SHRob, p=0.013). Liver B-cell lymphoma-2 protein (Bcl-2) levels (**Table 2**, **Fig. 2E**) were significantly decreased in SHRob (-90% versus controls: p=0.002) and were not altered after RDN.

Interstitial and perivascular collagen deposition, as determined by Picro-Sirius Red Staining (**Fig. 2F**), were significantly increased in SHRob (**Table 2**, **Fig. 2G**; +66% in SHRob versus controls, p<0.0001) and attenuated after RDN (**Table 2**). Western blot analysis for collagen type I content confirmed a corresponding increase in collagen type I in SHRob (+248%, p=0.0006 versus controls), which was reduced after RDN (**Table 2**, **Fig. 2H**). Collagen type III was decreased in SHRob compared to controls and showed no further regulation after RDN (**Fig. 2I**).

Renal denervation and liver RAGE/sRAGE regulation: Hepatic RAGE expression assessed by Western blot analysis (**Fig. 3A**) was markedly increased in SHRob as compared to normotensive controls (**Table 2**, **Fig. 3B**: +426% in SHRob versus controls, p<0.0001). RDN lowered liver RAGE expression (-35% versus SHRob, p=0.018). sRAGE liver content on the other hand was significantly decreased in SHRob as compared to controls (**Table 2**, **Fig. 3C**; -89% in SHRob versus controls, p<0.0001) while in SHRobRDN sRAGE levels significantly increased (+302% versus SHRob, p=0.009). Levels of the RAGE splice variant esRAGE (endogenous secretory RAGE) were unaltered between the groups (**Table 2, Fig. 3D**). Immunofluorescent staining for RAGE in liver cross-sections revealed a robust RAGE signal mainly in hepatocytes (**Fig. 3E**). Liver sRAGE expression showed a negative correlation with collagen I protein content (**Fig. 3F**, right panel;

r= -0.782, p=0.011, n=10 SHRob and SHRobRDN) while RAGE-expression correlated positively (**Fig. 3F**, left panel; r= 0.964, p<0.0001, n=10 SHRob and SHRobRDN). Also, liver BAX expression showed a strong positive correlation with RAGE expression (**Fig. 3G**, left panel; r= 0.85, p=0.002, n=10 SHRob and SHRobRDN) and a negative correlation with liver sRAGE (**Fig.3G**, right panel; r= -0.78, p=0.02, n=10 SHRob and SHRobRDN).

Renal denervation and RAGE-ligands CML and HMGB1: Western blot analysis demonstrated significantly increased contents of the AGE carboxymethyllysine (CML) in SHRob liver tissue (**Table 2**, **Fig. 3H**). RDN resulted in a significant reduction of hepatic CML content (**Fig. 3H**; -39% versus SHRob, p=0.034). The RAGE ligand HMGB1, as assessed by Western blot analysis (**Fig. 3I,** upper panel), was increased in liver tissue from SHRob (**Table 2**, **Fig. 3I**). RDN also resulted in a significant reduction of HMGB1 protein expression (**Fig. 3I,** lower panel; -71% versus SHRob, p=0.013) reaching similar HMGB1 levels as in normotensive controls.

Renal denervation and RAGE cleaving proteases ADAM-10 (A-Disintegrin-And-Metalloproteinase-10) and MMP-9 (Matrix-Metalloproteinase-9) and their inhibitor TIMP-1 (Tissue-Inhibitor-of-Matrix-Metalloproteinases-1): Liver TIMP-1 protein expression (**Fig. 3J**) was significantly increased in SHRob compared to normotensive controls (**Table 2**, **Fig. 3J**; +85% in SHRob versus controls, p=0.002). TIMP-1 levels decreased after RDN (**Fig. 3J**: -52% versus SHRob, p=0.0007) and correlated positively with RAGE-expression (**Fig. 3K**, left panel; r= 0.83, p=0.005, n=10 SHRob and SHRobRDN) and inversely with sRAGE (**Fig. 3K**, right panel; r= -0.83, p=0.0047, n=10 SHRob and SHRobRDN). Accordingly, ADAM-10 activity was significantly decreased in SHRob (**Table 2**, **Fig. 3L**: -73% in SHRob versus controls, p=0.0016). Proteolytic activity of ADAM-10 recovered after RDN (+171% increase versus SHRob, p=0.032). Latent MMP-9 protein (**Table 2**, **Fig. 3M**) was not influenced by RDN and there was almost no active MMP-9 detectable throughout the groups (**Fig. 3M**, upper panel).

Cell culture experiments

ß-adrenergic stimulation of HepG2 cells: HepG2 cells were repeatedly stimulated with the ß1+ß2-adrenoreceptor agonist isoproterenol (0.1 µmol/l every 24 hours), which significantly increased the RAGE content in the cell membrane (**Fig. 4A**; +70% increase). The sRAGE shedding into the cell culture medium was simultaneously reduced by isoproterenol treatment with a significant reduction after 72h hours (-56% reduction; **Fig. 4B**). To identify the ß-adrenergic receptor subtype responsible for the observed effects, we also investigated RAGE/sRAGE expression in the presence of ß-adrenergic receptor antagonists with different selectivities (CGP 201712A (ß1-selective) or ICI 118.551 (ß2-selective)) and simultaneous isoproterenol stimulation. Isoproterenol treatment increased lipid accumulation as depicted by ADRP expression in HepG2 cells (**Fig. 4C**). Both the isoproterenol-induced RAGE expression (**Fig. 4A**) and lipid accumulation (**Fig. 4C**), was reversed by the ß1-adrenergic receptor blockade with CGP. Especially one hour pre-treatment of HepG2 cells with sRAGE almost completely prevented the isoproterenol-induced intracellular lipid accumulation (**Fig. 4D**, **E** and **F**).

Human data

sRAGE regulation in RDN responders: Table 3 depicts patients´ baseline characteristics. In order to validate and translate the observed effects of RDN from our SHRob animal model, where plasma ALT activities correlated with liver RAGE/sRAGE content (**Fig. 5A and B**), to human subjects, we investigated plasma sRAGE development in association with liver transaminase enzyme activities over a period of 6 months in 20 patients undergoing catheter-based RDN. In RDN-responders, 24h-systolic blood pressure significantly decreased 6 months after RDN by 21/9 mmHg (**Fig. 5C**). sRAGE plasma levels increased after RDN at 6-month follow-up (**Fig. 5D**: +21%, p=0.007). ALT values were increased in only 6 patients (30%) but decreased significantly during follow-up (**Fig. 5E**). Delta ALT correlated negatively with body mass index (BMI) (**Fig. 5F**) and delta sRAGE correlated negatively with delta ALT (**Fig. 5G**).

Discussion

NAFLD with resulting NASH represent an increasing burden for health care systems (**24**). This study provides evidence for sympathoadrenergic-dependent regulation of the ligand-RAGE/sRAGE axis in vivo and in vitro with liver remodeling and the development of fatty liver. In a rat model for hypertension and metabolic syndrome, effective sympathetic modulation by RDN reflected by a reduction of renal norepinephrine tissue content was accompanied by a decrease in liver norepinephrine tissue content and lower liver tyrosine hydroxylase activity. This extends findings in the heart, where RDN led to reduced cardiac sympathetic innervation and activity (**25**) accompanied by improvements in left ventricular hypertrophy (**26**). This implies a systemic effect of RDN on overall sympathoadrenergic activity and norepinephrine spillover, thereby impacting disease-specific phenotypes of other organs under conditions of increased sympathetic activation.

In this study, we further demonstrate an increase in hepatic lipid content in SHRob and a significant reduction of hepatic steatosis after RDN, using histological analysis and expression of ADRP (adipose-differentiation-related-protein), a marker of lipid droplet accumulation (**27**). Both ß1-, ß2- and ß3-AR subtypes are present in liver tissue of humans and rodents and have been shown to be involved in the regulation of age-dependent hepatic fat accumulation (**28-29**). A reduction of ß-AR stimulation by reduced catecholamines might also be involved in the anti-steatotic effects after RDN observed herein, although liver ß-AR expression per se was not altered after renal denervation. As proof of concept, we treated HepG2 cells with isoproterenol and showed increased cellular lipid accumulation and cellular RAGE expression, which could both be prevented by ß1-adrenergic blockade. Interestingly, isoproterenol-induced lipid accumulation in HepG2 cells could also be prevented by pretreatment with a physiological concentration of recombinant sRAGE. This suggests an involvement of RAGE in ß-adrenoreceptor augmented lipid droplet formation and development of fatty liver, which, of note, requires intact lipid balance related mechanisms, as it did not work in $ApoE^{-}/LDLR^{-}$- double-knockout mice (**30**).

In SHRob, fibrosis was reduced by RDN, as reflected by the reduction in hepatic collagen content. Liver BAX expression was increased in SHRob as compared to controls, indicating increased hepatic injury and liver cell death, which in turn has been implicated in the development of hepatic fibrosis (**31-32**). BAX expression positively correlated with RAGE expression and showed a negative correlation with liver sRAGE, while RAGE/sRAGE correlated with collagen I. These findings demonstrate the association of liver cell death and fibrosis and suggest a link to RAGE/sRAGE (**33-34**). RDN modulates liver RAGE/sRAGE in SHRob to a favourable anti-inflammatory balance by decreasing RAGE, increasing sRAGE levels and decreasing liver ALT. Plasma sRAGE levels have been shown to be associated with a number of risk factors for MetS in non-diabetic otherwise healthy individuals (**10**) and to play protective roles in patients with NAFLD **(6)**.

Morphometric evaluation of immunofluorescent staining for RAGE in our rat liver samples indicates mainly hepatocyte RAGE expression. Hepatic stellate cells (HSC), however, have also been shown to express RAGE (**34**). In models with more profound liver fibrosis and inflammation like NASH, they probably play an important role as RAGE-mediated NADPH oxidase-derived reactive oxygen species could contribute to hepatic fibrosis via activation of HSCs (**34**) and to increase hepatic steatosis (**35-36**). Furthermore, in different pathologies, RAGE/sRAGE balance is not only influenced by an increase in RAGE production, but also by decreased RAGE cleavage. ADAM-10 (A Disintegrin and Metalloproteinase-10) and MMP-9 (Matrix Metalloproteinase-9) are the only proteases known to cleave RAGE, the process being accompanied by sRAGE accumulation as the cleavage product being shedded from the cell surface (**14-15**). TIMP-1 is a potent protease inhibitor for both ADAM-10 and MMP-9 and shows distinct induction in SHRob livers. Herein, TIMP-1 upregulation is accompanied by a decrease in ADAM-10 activity, which partially recovers after RDN. TIMP-1 is also reduced by RDN in this study. Interestingly, we could not observe substantial MMP-9 activation in any of the rat groups. This may indicate that MMP-9 activity is not critical for mediating RAGE cleavage in this model.

Also, RDN decreases the levels of the RAGE-activating ligands CML and HMGB1 in SHRob, which both have been demonstrated to be increased in fatty livers (**37-38**). The AGE/RAGE-axis is known to induce and

augment hepatic insulin resistance (**39-40**). RDN improved RAGE/sRAGE-balance and decreased liver CML-levels in our rat model, which was associated with attenuation of hyperinsulinemia. Beneficial effects of RDN on glucose metabolism have also been described in patients previously (**23**). Our study shows increased HMGB1 liver content in SHRob. HMGB1 released from NAFLD liver has been described to reach other organs and to bind to RAGE receptors inducing oxidative stress and transcription of inflammatory cytokines (**41**). HMGB1 has also been suggested as a biomarker for acute liver cell death (**31**). Damaged hepatocytes have been reported to release HMGB1, which then interacts with RAGE in the pathogenesis of HSCs activation and liver fibrosis (**42-43**). Engagement of RAGE with RAGE ligands increases expression of RAGE itself in a variety of cells (**35, 44-45**). These positive feedback loops could partly explain why RAGE ligands interaction leads to sustained activation of the RAGE downstream pathway, contributing to the progression of chronic liver disease (**34**).

We further explored whether similar RDN-mediated effects occur in hypertensive patients with documented blood pressure falls following catheter-based RDN and assessed sRAGE plasma levels. We detected a significant increase in plasma sRAGE at 6 months after RDN consistent with the sRAGE regulation seen in livers from SHRobRDN rats in this study and also with sRAGE plasma and cardiac levels reported in the same rat model in a previous study from our laboratory (**46**). ALT values in SHRob rats correlated strongly with liver RAGE-expression. Correspondingly, there was a decrease in ALT plasma concentrations during follow-up in our patients. Changes in ALT activity correlated with sRAGE-changes. NAFLD is the most common cause for an isolated increase in ALT values among adults, which has been discussed as a marker of NAFLD (**47**). The correlation between ALT changes and plasma sRAGE changes in our patients is a hint, although not proof, for RDN-induced sRAGE mediated anti-steatotic effects on liver.

There are potential limitations to our study that deserve mentioning. Our SHRob model displayed a robust steatosis with beginning fibrosis, but no NASH. RDN induced alterations could have been even more profound in a NASH-model with marked fibrosis and inflammation. Also, a longer observation time than 3 months after RDN might have resulted in more striking effects. The secondary evaluation of sRAGE plasma levels in

patients is limited because the primary indication for RDN was arterial hypertension and not hepatosteatosis or liver disease. Consequently, we have no assessment of liver histopathology in our patients. The mean BMI in all patients was high, which usually goes along with hepatosteatosis (**47-48**) and changes in ALT activity. The correlations presented should therefore be considered hypotheses generating.

In conclusion:

Renal denervation reduces hepatic steatosis and liver injury in SHRob with MetS and is associated with an improved liver RAGE/sRAGE balance. These findings suggest treatment effects by RDN on NAFLD, that is renal afferent disruption alters sympathetic innervation to the liver and influences clinically relevant phenotypes such as hepatic fat deposition and fibrosis. RDN in hypertensive patients with decreases in systolic blood pressure, increases plasma sRAGE, which is associated with a reduction in plasma ALT activity as a marker of NAFLD. This sets the stage for further experimental and clinical studies to reduce the burden of metabolic liver disease by modulation of the sympathetic nervous system.

Materials and Methods

ANIMAL MODEL

Animals

Male obese spontaneously hypertensive rats (SHRob, n=10), a strain displaying a natural leptin receptor knockout (**22**), and normotensive lean control rats (Sprague-Dawley, n=5) were purchased at an age of ten weeks from Charles River (Sulzfeld, Germany). The animals were housed individually in standard cages, receiving standard chow diet (standard diet #1320, Altromin, Lage, Germany) and tap water ad libitum. Animals were treated in accordance with the National Instructions of Health (NIH) Guide for the Care and Use of Laboratory Animals and with the Welfare guidelines and the German law for the protection of animals. The study was approved by the regional commission in charge.

Renal denervation procedure (RDN)

RDN was performed in SHRob at the age of 32 weeks (SHRobRDN) to investigate the role of renal sympathetic innervation on the development of hepatic end-organ damage. Both kidneys were approached through medial laparotomy and retroperitoneal incisions under general anesthesia with 2.5% isoflurane. Renal denervation was performed on both kidneys by cutting the visible nerves in the area of the renal hilum and stripping from the adventitia of the renal arteries, which was followed by moistening the area with a 20% phenol/ethanol solution as described previously (**21**). Sham-operations were performed on SHRob and controls in comparison with SHRobRDN. Implantation of telemetric sensors (TL11M2-C50-PXT PMP, Data Sciences International, St. Paul, MN) acquiring systolic and diastolic blood pressure and heart rate for 100 days, was performed simultaneously with the RDN procedure (**21**). For analysis and data plotting a Fourier-transformation was applied to the raw data using the vendor software (Dataquest A.R.T., V4.0) as described before (**20-21**).

Measurement of blood parameters

Blood samples were obtained for metabolic characterization from the retro-orbital plexus under light anesthesia (3.5% isoflurane) at the age of 42 weeks. Blood glucose and glycated hemoglobin (HbA1c) were measured using standard kits (Cobas Integra, Roche Diagnostics, Mannheim, Germany). Also, oral glucose tolerance testing was performed at the time.

Cardiac invasive and functional measurements

At 45 weeks of age, cardiac LV-function was assessed by cardiac magnetic resonance imaging (MRI), followed by invasive LV-pressure measurements under anesthesia (**21**). Afterwards the animals were sacrificed as described before (**20-21**).

Asservation of blood and tissue samples

After completion of invasive functional measurements, blood was extracted from the aorta and stored at -80°C until further analysis. Livers were rapidly removed and exsanguinated, aliquots of liver tissue were snap-

frozen in liquid nitrogen and stored at -80°C. Finally, the animals were sacrificed by quick excision of the hearts under continued deep anesthesia. Kidney and liver tissues were used for norepinephrine measurement by high-pressure-liquid-chromatography (HPLC) as described before (**21**).

Histopathological analysis of liver tissue

A part of the right liver lobe was resected and fixed in buffered 4% paraformaldehyde for 24 hours and embedded in paraffin for histopathological evaluation. Liver cross sections were cut at 3 µm, deparaffinized, rehydrated, and stained with hematoxylin and eosin (#2C-163, Waldeck, Münster, Germany) for morphometric evaluation and with Picro-Sirius Red (#13422.00500, Morphisto, Frankfurt am Main, Germany) for fibrillar collagen. The fractional area of collagen content in liver tissue was measured with the image analysis software Lucia G (Nikon, Düsseldorf, Germany). Hepatic steatosis was scored in a blinded fashion by a previously described method (**49**): Liver samples with no appreciable fat droplets were scored grade 0, tissues with few small fat droplets near the portal region defined grade 1, many fat droplets of moderate size near midzonal and portal regions received grade 2, and many large fat droplets distributed throughout the tissue sample were scored grade 3.

Immunofluorescence analysis for liver RAGE

To detect RAGE expression, RAGE immunostainings on 3 µm paraffin sections of liver tissue were performed using heat-mediated antigen retrieval with 0.05% citraconic anhydride solution followed by overnight incubation at 4 °C with the 1:100 diluted primary antibody (Abcam; ab37647, rabbit polyclonal to RAGE) and incubation with the appropriate secondary antibody (TRITC-conjugated anti-rabbit IgG (Dianova, Germany)) at 37 °C for 1 h (dilution 1:30). 1xPBS buffer with 0.1% Tween 20 was used for washing steps. Sections were counterstained with DAPI (Calbiochem, Germany) and mounted with fluorescent mounting medium (Vectashield, Vector Laboratories, USA) for fluorescence microscopic analysis. All sections were evaluated using a Nikon Eclipse epifluorescence microscope (Nikon, Germany) with appropriate filters at 100x and 400x magnification.

Western blot

Human plasma samples were diluted 1:50 and rat liver samples were homogenized with extraction buffer (10 mmol/l cacodylic acid (pH 5.0), 0.15 mol/l NaCl, 1 µmol/l ZnCl2, 20 mmol/l CaCl2, 1.5 mmol/l NaN_3, and 0.01% (v/v) Triton X-100) and mixed 2:1 v/v with SDS-PAGE loading buffer. The samples were denatured (95°C, 5 min), separated on 10-12% SDS polyacrylamide electrophoresis gels (liver tissue 25 µg/lane, diluted plasma samples 10 µl/lane), and transferred to nitrocellulose membranes (Protran®, Schleicher & Schuell GmbH, Dassel, Germany) by semi-dry electrophoretic blotting and subjected to Western blot analysis. Membranes were blocked with 0.1% Western Blocking Reagent (Roche, Mannheim, Germany) followed by incubation with primary antibodies for RAGE/sRAGE (ab37647, rabbit polyclonal to RAGE, 1:1000 dilution, Abcam, Cambridge, UK), HMGB1 (ab18256, rabbit polyclonal to HMGB1, 1:1000, Abcam), CML (ab 27684, rabbit polyclonal to CML, 1:2000, Abcam), BAX (sc-7480, mouse monoclonal to BAX, 1:1000, Santa Cruz), Bcl-2 (sc-492, rabbit polyclonal to Bcl-2, 1:1000, Santa Cruz), tyrosine hydroxylase (ab112, rabbit-monoclonal, 1:1000, Abcam) and phospho-S40-tyrosine hydroxylase (ab51206, rabbit-polyclonal, 1:1000, Abcam), ADAM-10 (ab1997, rabbit polyclonal to active and latent ADAM-10, 1:1000, Abcam), MMP-9 (IM 10L, rabbit polyclonal to active and latent MMP-9, 1:1000, Calbiochem), TIMP-1 (IM32L, mouse monoclonal to TIMP-1, 1:1000, Calbiochem), Collagen I (1310-01, goat-anti-collagen type I, 1:1000, Southern Biotech), Collagen III (1330-01, goat-anti-collagen type III, 1:1000, Southern Biotech), ADRP (10R-A117A, mouse monoclonal to ADRP 1:1000, Fitzgerald) at 4°C for 12-16h. The goat anti-rabbit, goat anti-mouse and rabbit anti-goat secondary antibodies were diluted 1:10000 and incubated for 60 min at RT. Proteins were visualized by enhanced chemiluminescence (Amersham Pharmacia Biotech, Freiburg, Germany). Membranes with liver tissue samples were stripped afterwards and analyzed for GAPDH as loading control: twice stripped for 15 minutes at 56°C with stripping buffer (62.5 nM Tris-HCl (pH 6.8), 2%SDS, 0.1 M 2-mercaptoethanol), then thoroughly washed with 1xPBS (in mmol/L: NaCl 170, KCl 33, Na2HPO4 40 and KH2PO4 18, pH 7.2) for at least one hour and blocked again in phosphate buffered saline (PBS) containing 5% nonfat dry milk for 120 min at room temperature. Autoradiographs were quantified by imaging densitometry and analysed by the "LabWorks 4.6"- Software (LabWorks Image Acquisition and Analysis Software, UVP BioImaging Systems,

Cambridge, UK). Data are presented as arbitrary units (AU) normalized to GAPDH and a control sample for liver samples or to plasma albumin concentrations for human plasma samples.

CELL CULTURE

HepG2 culture conditions

Human hepatoma HepG2 cells (Sigma-Aldrich, Germany) were cultured on uncoated 6-well dishes in 2ml DMEM medium +10%FBS in humidified air (5% CO2) at 37°C until 80% confluency, then the cell culture medium was replaced by a low FBS hunger medium (0.1% FBS) for 24 hours, followed by a 72 hours stimulation period with isoproterenol (0.1 umol/l) in the presence or absence of ß-adrenergic receptor antagonists with differing selectivity (ß1-selective CGP 201712A, ß2-selective ICI 118.551; Sigma-Aldrich Germany) or recombinant sRAGE (5 ng/ml; BioVendor, Germany).

Cell fractionation and Western blotting

The cell culture supernatant of the stimulated HepG2 cells was asserved every 24 hours for 3 days and examined for sRAGE release. The HepG2 cells were harvested after 72 hours of stimulation and further processed for cell fractionation and Western blotting. The cells were washed with ice-cold PBS, pH 7.4 and cell pellets resuspended in hypotonic buffer (in mmol/l: Tris 5, EDTA 1, MgCl2 5, pH 8.0, PMSF 1, Leupeptin 1; Aprotinin 5 ug/ml). After incubation for 15 minutes at 4°C, cell pellets were subjected to 100000 g ultracentrifugation (1h, 4 °C) to obtain a "cytosolic" (supernatant) and "membranous" fraction (pellet).

The membrane fraction was resuspended in 100 µl hypotonic buffer. Membrane fraction and cell culture supernatant were analyzed for RAGE/sRAGE content by Western blot analysis, cell homogenates for ADRP protein regulation. The uniform total protein loading on the gel (50 µg/lane) was controlled by Ponceau Red staining (Dianova, Germany) for membrane fraction and GAPDH for homogenates. The data are presented as arbitrary units (AU) in percent of a control, unless otherwise stated.

Cell fixing and Oil Red staining

72 hours after repeated stimulations (every 24 hours), HepG2 cells were fixed in 10% (v/v) formaldehyde for at least 2h at room temperature. Afterwards, fixed cells were rinsed in distilled water, permebealized with 0.1% PBS-Tween and then stained with Oil Red solution for lipid staining for 2hours, followed by a wash step with aqua dest. Photographic images were taken of three random fields of each stained specimen using a Nikon E600 epifluorescence microscope (Nikon, Germany).

Cell fixing and ADRP immunofluorescence staining

Cells were washed two times with 1ml PBS (NaCl 137 mM, KCl 2.7 mM; Na2HPO4 10mM, KH2PO4 7,4mM) after which 100 µl of 4% paraformaldehyde (PFA) solution was added. Cells were fixed for 10 minutes at room temperature followed by 2 washes using PBS. Cells were stained for ADRP (Abcam, ab52356, 1:500 dilution) at room temperature overnight followed by 3 washes with 0.1% PBS-Tween, incubation with a FITC-labeled anti-rabbit secondary antibody for 2 hours, 3 washes with 0.1% PBS-Tween and 2 washes with PBS, then mounted with fluorescent mounting medium with DAPI (Vectashield, Vector Laboratories, USA). Prepared plates were kept at 4°C and protected from light prior to imaging. Random sections were evaluated using a Nikon E600 epifluorescence microscope (Nikon, Germany).

HUMAN DATA

Renal denervation in hypertensive patients

Plasma samples from 20 consecutive patients, who underwent bilateral renal denervation (RDN) and were classified as "RDN-responders" from the Symplicity Extension Study (NCT 01888315) enrolled between October 2012 and February 2014 were assessed for plasma sRAGE levels. The included patients had resistant hypertension according to the guidelines of the European Society of Hypertension/European Society of Cardiology: Systolic blood pressure (SBP) ≥ 140 mmHg despite treatment with at least three antihypertensive drugs including a diuretic. Hypertension was confirmed by 24-hour ambulatory blood pressure measurements (ABPM). Physical examination and blood pressure measurements were performed at baseline and follow-up visits, as well as a blood sampling at baseline and at subsequent follow-up after 6 months. The glomerular filtration rate (GFR) was determined by cystatin C measurements. ABPM were performed with an automated

oscillometric device (Spacelabs 90207, Spacelabs Healthcare, Snoqualmie, Washington, USA) according to current guidelines (**50**). An adequate response to RDN was defined as a reduction of systolic ambulatory blood pressure ≥5 mmHg in 24h-ABPM after 6 months (**51**). RDN was performed with a mono-electrode radiofrequency catheter (Symplicity Flex, Medtronic Vascular, Santa Rosa, California, USA). All procedures were performed by experienced interventionalists (≥ 10 RDN procedures per year). All patients had given written informed consent and the study was approved by the local ethics committee.

Statistical analysis

Data are expressed as mean ± SEM. Statistical significance was estimated with 2-way-ANOVA with post-hoc-tests, as appropriate. The statistical analyses were corrected for multiple comparisons. Normal distribution of data was tested by Kolmogorov-Smirnov and Lilliefors test, correlation analyses were performed using Spearman rank correlation coefficients or Pearson´s correlations where appropriate. Follow-up measurements in patients were analyzed with a paired t-test. A probability value <0.05 was considered significant. Statistical analysis was performed with Graph Pad Prism (version 5.0; GraphPad Software, San Diego California, USA).

Acknowledgements

The authors thank Laura Frisch for excellent technical assistance.

Author contributions

SRS and DL designed and performed experiments, analyzed data and wrote the manuscript. JD, AK and OZ performed experiments and analyzed data. MH, TS, MK, FL, LL, FM and MB designed research, contributed new reagents and analytic tools and wrote the manuscript.

Funding

This work was supported by HOMFOR 2015/2016 to SRS, the German Heart Foundation (F/03/15 to SRS and DL), the Federal Ministry for Education and Research (BMBF, LiSyM 031L0051 to FL) and the German

Research Foundation (Deutsche Forschungsgemeinschaft, SFB/TRR 219 to SRS, DL, MH, AK, TS and MB (M02/S02, S01, M06, C08)).

Conflict of interest

M.B. has received speaker honoraria for lectures and scientific advice from Abbott, AstraZeneca, Boehringer Ingelheim, Medtronic, Servier, Vifor and Novartis outside of the submitted work. F.M. received speaker honoraria from Medtronic and Recor, and is supported by Deutsche Hochdruckliga, Deutsche Gesellschaft für Kardiologie and Deutsche Forschungsgemeinschaft.

References

1. Reccia I, et al. (2017) Non-alcoholic fatty liver disease: A sign of systemic disease. *Metabolism*. 72: 94-108.

2. Fabbrini E, et al. (2009) Intrahepatic fat, not visceral fat, is linked with metabolic complications of obesity. *Proc Natl Acad Sci U S A.* 106: 15430-15435.

3. Stefan N, Kantartzis K, Haring HU. (2008) Causes and metabolic consequences of fatty liver. *Endocrine Reviews*. 29: 939–960.

4. Liang JQ, et al. (2018) Dietary cholesterol promotes steatohepatitis related hepatocellular carcinoma through dysregulated metabolism and calcium signaling. *Nat Commun.* 9: 4490.

5. Kumashiro N, et al. (2011) Cellular mechanism of insulin resistance in nonalcoholic fatty liver disease. *Proc Natl Acad Sci U S A*. 108: 16381-16385.

6. Zelber-Sagi S, et al. (2017) Protective role of soluble receptor for advanced glycation end-products in patients with non-alcoholic fatty liver disease. *Dig Liver Dis.* 49: 523-529.

7. Böhm M, Linz D, Urban D, Mahfoud F, Ukena C. (2013) Renal sympathetic denervation: applications in hypertension and beyond. *Nat Rev Cardiol*. 10: 465-476.

8. Huh JH, et al. (2017) An association of metabolic syndrome and chronic kidney disease from a 10-year prospective cohort study. *Metabolism.* 67: 54-61.

9. Gaens KH, Stehouwer CD, Schalkwijk CG. (2013) Advanced glycation endproducts and its receptor for advanced glycation endproducts in obesity. *Curr Opin Lipidol.* 24: 4-11.

10. Sebeková K, Krivošíková Z, Gajdoš M. (2014) Total plasma Nε-(carboxymethyl)lysine and sRAGE levels are inversely associated with a number of metabolic syndrome risk factors in non-diabetic young-to-middle-aged medication-free subjects. *Clin Chem Lab Med.* 52: 139-149.

11. Schmidt AM, et al. (1994) Receptor for advanced glycation end products (AGEs) has a central role in vessel wall interactions and gene activation in response to circulating AGE proteins. *Proc Natl Acad Sci U S A*. 91: 8807-8811.

12. Wautier JL, et al. (1994) Advanced glycation end products (AGEs) on the surface of diabetic erythrocytes bind to the vessel wall via a specific receptor inducing oxidant stress in the vasculature: a link between surface-associated AGEs and diabetic complications. *Proc Natl Acad Sci U S A.* 91: 7742-7746.

13. Sárkány Z, et al. (2011) Solution structure of the soluble receptor for advanced glycation end products (sRAGE*). J Biol Chem*. 286: 37525-37534.

14. Raucci A, et al. (2008) A soluble form of the receptor for advanced glycation endproducts (RAGE) is produced by proteolytic cleavage of the membrane-bound form by the sheddase a disintegrin and metalloprotease 10 (ADAM10). *FASEB J.* 22: 3716-3727.

15. Zhang L, et al. (2008) Receptor for advanced glycation end products is subjected to protein ectodomain shedding by metalloproteinases. *J Biol Chem*. 283: 35507–35516.

16. Hudson BI, et al. (2014) Serum levels of soluble receptor for advanced glycation end-products and metabolic syndrome: the Northern Manhattan Study. *Metabolism.* 63: 1125-1130.

17. Palma-Duran SA, et al. (2018) Serum levels of advanced glycation end-products (AGEs) and the decoy soluble receptor for AGEs (sRAGE) can discriminate non-alcoholic fatty liver disease in age-, sex- and BMI-matched normo-glycemic adults. *Metabolism*. 83: 120-127.

18. Böhm M, et al (2015) GSR Investigators. First report of the Global SYMPLICITY Registry on the effect of renal artery denervation in patients with uncontrolled hypertension. *Hypertension.* 65: 766-774.

19. Kandzari DE, et al; SPYRAL HTN-ON MED Trial Investigators. (2018) Effect of renal denervation on blood pressure in the presence of antihypertensive drugs: 6-month efficacy and safety results from the SPYRAL HTN-ON MED proof-of-concept randomised trial. *Lancet*. 391: 2346-2355.

20. Linz D, et al. (2012) Cardiac remodeling and myocardial dysfunction in obese spontaneously hypertensive rats. *J Transl Med.* 10: 187.

21. Linz D, et al. (2015) Progression of kidney injury and cardiac remodeling in obese spontaneously hypertensive rats: the role of renal sympathetic innervation. *Am J Hypertens*. 28: 256-265.

22. Ernsberger P, Koletsky RJ, Friedman JE. (1999) Molecular pathology in the obese spontaneous hypertensive Koletsky rat: a model of syndrome X. *Ann N Y Acad Sci.* 892: 272-288.

23. Mahfoud F, et al. (2011) Effect of renal sympathetic denervation on glucose metabolism in patients with resistant hypertension: a pilot study. *Circulation.* 123: 1940-1946.

24. Estes C, et al; NAFLD / NASH Working Group. (2018) Modeling NAFLD Disease Burden in China, France, Germany, Italy, Japan, Spain, United Kingdom, and United States for the period 2016-2030. *J Hepatol.* 69: 896-904.

25. Donazzan L, et al. (2016) Effects of catheter-based renal denervation on cardiac sympathetic activity and innervation in patients with resistant hypertension. *Clin Res Cardiol.* 105: 364-371.

26. Mahfoud F, et al. (2014) Effect of renal denervation on left ventricular mass and function in patients with resistant hypertension: data from a multi-centre cardiovascular magnetic resonance imaging trial. *Eur Heart J.* 35: 2224-2231.

27. Mak KM, Ren C, Ponomarenko A, Cao Q, Lieber CS (2008) Adipose differentiation-related protein is a reliable lipid droplet marker in alcoholic fatty liver of rats. *Alcohol Clin Exp Res.* 32: 683-689.

28. Ghosh PM, et al. (2012) Role of β-adrenergic receptors in regulation of hepatic fat accumulation during aging. *J Endocrinol.* 213: 251-261.

29. Shi Y, et al. (2017) Altered expression of hepatic β-adrenergic receptors in aging rats: implications for age-related metabolic dysfunction in liver. *Am J Physiol Regul Integr Comp Physiol.* 314: R574-R583.

30. Bijnen M, et al. (2018) RAGE deficiency does not affect non-alcoholic steatohepatitis and atherosclerosis in Western type diet-fed Ldlr-/- mice. *Sci Rep.* 8: 15256.

31. Eguchi A, Wree A, Feldstein AE. (2014) Biomarkers of liver cell death. *J Hepatol.* 60: 1063-1074.

32. Canbay A, Friedman S, Gores G.J. (2004) Apoptosis: the nexus of liver injury and fibrosis. *Hepatology*. 39: 273-278.

33. Nakamura K, Adachi H, Matsui T, Kurita Y, Takeuchi M (2009) Independent determinants of soluble form of receptor for advanced glycation end products in elderly hypertensive patients. *Metabolism.* 58: 421-425.

34. Yamagishi S, Matsui T. (2015) Role of receptor for advanced glycation end products (RAGE) in liver disease. *Eur J Med Res*. 20: 15.

35. Kim SY, et al. (2017) Pro-inflammatory hepatic macrophages generate ROS through NADPH oxidase 2 via endocytosis of monomeric TLR4-MD2 complex. *Nat Commun.* 8: 2247.

36. Cordero-Herrera I, et al. (2019) AMP-activated protein kinase activation and NADPH oxidase inhibition by inorganic nitrate and nitrite prevent liver steatosis. *Proc Natl Acad Sci U S A*. 116: 217-226.

37. Pereira ENGDS, et al. (2017) Hepatic microvascular dysfunction and increased advanced glycation end products are components of non-alcoholic fatty liver disease. *PLoS One.* 12: e0179654.

38. Gaens KH, et al. (2012) Endogenous formation of Nε-(carboxymethyl)lysine is increased in fatty livers and induces inflammatory markers in an in vitro model of hepatic steatosis. *J Hepatol.* 56: 647-655.

39. Yoshida T, et al. (2008) Telmisartan, an angiotensin II type 1 receptor blocker, inhibits advanced glycation end-product (AGE)-elicited hepatic insulin resistance via peroxisome proliferator-activated receptor-gamma activation. *J Int Med Res*. 36: 237-243.

40. Tahara N, et al. (2012) Serum levels of advanced glycation end products (AGEs) are independent correlates of insulin resistance in nondiabetic subjects. *Cardiovasc Ther.* 30: 42-48.

41. Chandrashekaran V, et al. (2017) HMGB1-RAGE pathway drives peroxynitrite signaling-induced IBD-like inflammation in murine nonalcoholic fatty liver disease. *Redox Biol.* 13: 8-19.

42. Hernandez C, et al. (2018). HMGB1 links chronic liver injury to progenitor responses and hepatocarcinogenesis. *J Clin Invest.* 128: 2436-2451.

43. Kao YH, et al. (2014) Involvement of the nuclear high mobility group B1 peptides released from injured hepatocytes in murine hepatic fibrogenesis. *Biochim Biophys Acta.* 1842: 1720–1732.

44. Sorci G, Riuzzi F, Giambanco I, Donato R. (2013) RAGE in tissue homeostasis, repair and regeneration. *Biochim Biophys Acta.* 1833: 101–109.

45. Abe R, Yamagishi S. (2008) AGE-RAGE system and carcinogenesis. *Curr Pharm Des.* 14: 940–945.

46. Selejan SR, et al. (2018) Sympathoadrenergic suppression improves heart function by upregulating the ratio of sRAGE/RAGE in hypertension with metabolic syndrome. *J Mol Cell Cardiol.* 122: 34-46.

47. Kim WR, Flamm SL, Di Bisceglie AM, Bodenheimer HC; Public Policy Committee of the American Association for the Study of Liver Disease. (2008) Serum activity of alanine aminotransferase (ALT) as an indicator of health and disease. *Hepatology.* 47: 1363-1370.

48. Woo Baidal JA, Lavine JE. (2016) The intersection of nonalcoholic fatty liver disease and obesity. *Sci Transl Med.* 8: 323rv1.

49. Maeda H, et al. (1985) Nutritional influences on aging of Fischer 344 rats: II. Pathology. *J Gerontol.* 40: 671-688.

50. Williams B, et al; ESC Scientific Document Group. (2018) 2018 ESC/ESH Guidelines for the management of arterial hypertension. *Eur Heart J.* 39: 3021-3104.

51. Mahfoud F, et al. (2017) Proceedings from the 2nd European Clinical Consensus Conference for device-based therapies for hypertension: state of the art and considerations for the future. *Eur Heart J.* 38: 3272-3281.

Figure legends:

Figure 1: Liver norepinephrine levels

A) Quantification of liver norepinephrine in liver homogenates from controls (n=5), SHRob (n=5) and SHRobRDN (n=5) by HPLC. *p<0.05 versus Control. #p<0.05 versus SHRob. **B**) Representative Western blot (upper panel) and quantification of tyrosine hydroxylase (TH) activity as phospho-TH/total TH ratio (lower panel) in liver homogenates from controls (n=5), SHRob (n=5) and SHRobRDN (n=5). #p<0.05 versus SHRob. **C**) Correlation between renal norepinephrine content and liver tyrosine hydroxylase activity in SHRob and SHRobRDN (n=10). Spearman correlation (p-value). **D**) Correlation between liver norepinephrine content and liver tyrosine hydroxylase activity in SHRob and SHRobRDN (n=10). Spearman correlation (p-value). **E)** Correlation between renal norepinephrine content and liver norepinephrine content in SHRob and SHRobRDN (n=10). Spearman correlation (p-value). **F)** Quantification of ß1-AR (upper panel), ß2-AR (middle panel) and ß3-AR (lower panel) by Western blot in liver homogenates from normotensive lean controls (n=5), SHRob (n=5) and SHRobRDN (n=5). ß1-AR, ß2-AR and ß3-AR in arbitrary units (AU) normalized to GAPDH. *p<0.05 versus Control.

Figure 2: Hepatic steatosis, fibrosis and liver injury

A) Representative histological pictures (Hematoxyllin-Eosin staining) in liver samples of control rats (upper panel), SHRob (middle panel) and SHRobRDN rats (lower panel) (n=5 each group). Magnification 100x. Scale bars 100 µm. **B**) Steatosis score in normotensive controls (n=5), SHRob (n=5) and SHRobRDN (n=5).

*p<0.05 versus Control; #p<0.05 versus SHRob. **C**) Representative Western blot (upper panel) and quantification of ADRP (lower panel) in liver homogenates from normotensive controls (n=5), SHRob (n=5) and SHRobRDN (n=5). ADRP in arbitrary units (AU) normalized to GAPDH. *p<0.05 versus Control; #p<0.05 versus SHRob.

Liver cell death as assessed by BAX/BCL: **D**) Representative Western blot (upper panel) and quantification of BAX (lower panel) in liver homogenates from normotensive controls (n=5), SHRob (n=5) and SHRobRDN (n=5). **E**) Representative Western blot (upper panel) and quantification of Bcl-2 (lower panel) in liver homogenates from normotensive controls (n=5), SHRob (n=5) and SHRobRDN (n=5). BAX and Bcl in arbitrary units (AU) normalized to GAPDH. *p<0.05 versus Control; #p<0.05 versus SHRob.

F) Representative histological pictures (Picro-Sirius Red staining) in liver samples of control rats (upper panel), SHRob (middle panel) and SHRobRDN rats (lower panel) (n=4 each group). Magnification 40x. Scale bars 100 μm. **G**) Quantification of liver interstitial and periportal/perivascular fibrotic area (%). *p<0.05 versus Control; #p<0.05 versus SHRob. **H**) Representative Western blot (upper panel; images from different parts of the same gel) and quantification of collagen type I (lower panel) in liver homogenates from normotensive controls (n=5), SHRob (n=5) and SHRobRDN (n=5). Collagen type I in arbitrary units (AU) normalized to GAPDH. *p<0.05 versus Control; #p<0.05 versus SHRob. **I**) Representative Western blot (upper panel) and quantification of collagen type III (lower panel) in liver homogenates from normotensive controls (n=5), SHRob (n=5) and SHRobRDN (n=5). Collagen type III in arbitrary units (AU) normalized to GAPDH.

Figure 3: Liver RAGE/sRAGE, RAGE-ligands (CML, HMGB1) and sRAGE shedding mechanisms.

A) Representative Western blot (images from different parts of the same gel) and **B**) quantification of RAGE and **C**) sRAGE in liver homogenates from controls (n=5), SHRob (n=5) and SHRobRDN (n=5). **D)** Representative Western blot (upper panel) and quantification of esRAGE (lower panel) in liver homogenates from controls (n=5), SHRob (n=5) and SHRobRDN (n=5). RAGE, sRAGE and esRAGE in arbitrary units (AU) normalized to GAPDH. *p<0.05 versus Control; #p<0.05 versus SHRob. **E**) Representative fluorescence microscopy for RAGE (red), hepatocyte autofluorescence (green) and nuclei (stained blue by DAPI) in liver

samples of control rats (left panel), SHRob (middle panel) and SHRobRDN rats (right panel) (n=4 each group). Magnification 100x. Scale bars 100 μm**. F**) Correlation between between liver RAGE and liver collagen I expression (left panel) and liver sRAGE content and liver collagen I expression (right panel) in SHRob and SHRobRDN (n=10). Spearman correlation (p-value). **G)** Correlation between liver BAX expression and liver RAGE expression (left panel) and between liver BAX expression and liver sRAGE expression (right panel) in SHRob and SHRobRDN (n=10). Spearman correlation (p-value). **H)** Representative Western blot of hepatic CML-modified proteins (upper panel) and quantification of CML (lower panel) in normotensive controls (n=5), SHRob (n=5) and SHRobRDN (n=5). CML in arbitrary units (AU) normalized to GAPDH. *p<0.05 versus Control; #p<0.05 versus SHRob. **I**) Representative Western blot of hepatic HMGB1 (upper panel) and quantification of HMGB1 (lower panel) in controls (n=5), SHRob (n=5) and SHRobRDN (n=5). HMGB1 in arbitrary units (AU) normalized to GAPDH. *p<0.05 versus Control; #p<0.05 versus SHRob. **J**) Representative Western blot (upper panel) and quantification of TIMP-1 in liver homogenates (lower panel) from controls (n=5), SHR (n=6), SHRob (n=5) and SHRobRDN (n=5). TIMP-1 in arbitrary units (AU) normalized to GAPDH. *p<0.05 versus Control; #p<0.05 versus SHRob. **K)** Correlation between liver TIMP-1 expression and liver RAGE expression (left panel) and between liver TIMP-1 expression and liver sRAGE expression (right panel) in SHRob and SHRobRDN (n=10). Spearman correlation (p-value). **L**) Representative Western blot (upper panel, images from different parts of the same gel) and quantification of active ADAM-10 (lower panel) in liver homogenates from controls (n=5), SHRob (n=5) and SHRobRDN (n=5). Active ADAM-10 in arbitrary units (AU) normalized to GAPDH. *p<0.05 versus Control; #p<0.05 versus SHRob. **M**) Representative Western blot (upper panel; images from different parts of the same gel) and quantification of latent MMP-9 protein (lower panel) in controls (n=5), SHRob (n=5) and SHRobRDN (n=5). MMP-9 in arbitrary units (AU) normalized to GAPDH. Latent MMP-9 from HT-1080 supernatant served as positive control.

Figure 4: RAGE expression and lipid accumulation in HepG2.

A) Representative Western blot (upper panel) and quantification of membrane RAGE expression in HepG2 cells (lower panel) repeatedly stimulated with isoproterenol (ISO) 0.1 umol/l (n=4) in the presence or absence

of CGP (ß1-selective antagonist; 0.3 umol/l) or ICI (ß2-selective antagonist; 0.1 umol/l) for 72h every 24h. RAGE expression in arbitrary units (AU) normalized to Ponceau red with the control sample assigned a value of 1. *p<0.05 versus Control and ISO+CGP. **B**) Representative Western blot (upper panel) and quantification of sRAGE secretion in supernatant of HepG2 cells (lower panel) repeatedly stimulated with isoproterenol (ISO) 0.1 umol/l (n=4) in the presence or absence of CGP (ß1-selective antagonist; 0.3 umol/l) or ICI (ß2-selective antagonist; 0.1 umol/l) for 72 h every 24h. sRAGE expression in arbitrary units (AU) normalized to cell protein with the control sample assigned a value of 1. #p<0.05 versus Control and ISO+ICI. **C**) ADRP accumulation in HepG2 cells repeatedly stimulated with isoproterenol (ISO) 0.1 umol/l (n=5-8) in the presence or absence of CGP (ß1-selective antagonist; 0.3 umol/l) or ICI (ß2-selective antagonist; 0.1 umol/l) for 72 h every 24h. Representative Western blot (upper panel) and quantification of ADRP in HepG2 cells (lower panel). *p<0.05 versus Control and ISO+CGP. **D**) Representative Western blot (upper panel) and quantification of ADRP in HepG2 cells (lower panel) repeatedly treated with recombinant sRAGE (5ng/ml) and isoproterenol (ISO) 0.1 umol/l (n=5-8) for 72h every 24h. sRAGE was added 1h before ISO stimulation. ADRP expression in arbitrary units (AU) normalized to GAPDH with the control sample assigned a value of 1. *p<0.05 versus Control and sRAGE+ISO. Lipid specific formation detected by lipid specific stains like **E**) Oil Red staining and **F**) ADRP (green fluorescence) immunofluorescent staining for ADRP and DAPI (blue) for nuclei staining. Scale bars 10 µm.

Figure 5: RDN effects on plasma sRAGE and ALT activity in hypertensive patients

A) Correlation between liver RAGE and plasma ALT activity in SHRob and SHRobRDN (n=10). Spearman correlation (p-value). **B**) Correlation between liver sRAGE and plasma ALT activity in SHRob and SHRobRDN (n=10). Spearman correlation (p-value). **C**) 6 months follow-up measurements of ambulant systolic blood pressure (ABP) in RDN responders (n=20). P-value as determined by paired t-test. **D**) Representative Western blot (upper panel) and 6 months follow-up quantification of plasma sRAGE (lower panel) in RDN responders (n=20). P-value as determined by paired t-test. **E**) 6 months follow-up measurement of plasma ALT activity in RDN responders (n=20). P-value as determined by paired t-test. **F**) Scatter plot

between BMI and ALT change in RDN-responders (n=20). Pearson correlation (p-value). **G**) Scatter plot between plasma sRAGE change and ALT change in RDN-responders (n=20). Pearson correlation (p-value).

Table 1: Metabolic parameters, left ventricular, renal and hepatic function

	Control n=5	**SHRob n=5-7**	**SHRobRDN n=5-8**	Control Vs. SHRob	SHRob Vs. SHRob RDN	Control Vs. SHRob RDN
Parameters				**P-value**		
Creatinine umol/l	22±1.1	27.0 ± 2.7	16.25 ± 2.5	0.296	**0.0186**	0.213
GFR l/kg/h	0.57±0.02	0.18 ± 0.03	0.37 ± 0.03	**<0.0001**	**0.0012**	**0.0011**
EF (%)	65.0±1.85	45.7 ± 1.6	54.1 ± 1.2	**0.0002**	**0.0294**	**0.0059**
LVedP mmHg	3.84±1.04	14.56 ± 2.6	5.8 ± 2.1	**0.02**	**0.046**	0.777
MAP mmHg	122±4.0	229±3.3	172± 12.3	**<0.0001**	**0.001**	**0.0013**
HR bpm	329±4.5	271±11.1	277±13.3	**0.0064**	0.93	**0.006**
Fasting Insulin Pg/ml	729±90.2	10626 ±1519	7930 ± 1254	**0.0002**	0.369	**0.0013**
Fasting Glucose mmol/l	4.9±0.2	5.98±0.17	5.13±0.37	0.074	0.128	0.871
HbA1C %	3.97%±0.02	3.66%±0.14	3.65% ± 0.15	0.15	0.999	0.18
Renal Norepinephrine pg/mg	90.5±14.7	96.9 ± 7.5	6.73 ± 1.9	0.817	**0.0009**	**0.0004**
Aspartate aminotransferase U/l	123 ± 8.7	120± 7.2	109± 12.2	0.984	0.767	0.616
Alanine aminotransferase U/L	62± 2	110± 8.7	70± 3.2	**<0.0001**	**0.0003**	0.512
Cholesterol mmol/l	3.73± 0.15	9.73± 0.4	9.56± 0.8	**<0.0001**	0.975	**<0.0001**
LDL mmol/l	1.13± 0.09	4.09± 0.3	3.59± 0.5	**0.0002**	0.554	**0.0005**
HDL mmol/l	1.69± 0.1	2.63± 0.12	2.91± 0.12	**0.0003**	0.214	**<0.0001**
Triglycerides mmol/l	1.55± 0.12	5.3± 0.4	4.93± 1.1	**0.028**	0.946	**0.029**

GFR: glomerular filtration rate; EF: left-ventricular ejection fraction; LVedP: Left-Ventricular end-diastolic Pressure; MAP: Mean Arterial Pressure; HR: Heart Rate; SHRob: Spontaneously Hypertensive Obese Rat; SHRobRDN: Spontaneously Hypertensive Obese Rat with renal denervation

Table 2: Liver interstitial fibrosis, steatosis, RAGE/sRAGE expression, RAGE-ligand levels (CML and HMGB1), liver cell injury and liver sympathoadrenergic system.

	Control n=5	**SHRob n=5-7**	**SHRobRDN n=5-8**	Control vs. SHRob	SHRob vs. SHRob RDN	Control vs. SHRob RDN
Parameters				**p-value**		
Liver fibrotic area %	0.74± 0.07	1.23 ± 0.01	0.92± 0.05	**<0.0001**	**0.0023**	0.056
Liver Collagen I AU/GAPDH	0.4 ± 0.09	1.39 ± 0.11	0.6± 0.2	**0.0006**	**0.005**	0.449
Liver Collagen III AU/GAPDH	2.78 ± 1.1	0.82 ± 0.11	0.66± 0.17	0.112	0.983	0.083
Liver steatosis Grading	0.36± 0.1	1.59± 0.17	0.65± 0.19	**0.0004**	**0.0024**	**0.499**
Liver ADRP AU/GAPDH	0.54± 0.05	2.08± 0.36	0.88± 0.36	**0.008**	**0.033**	0.71
Liver sRAGE AU/GAPDH	3.81± 0.3	0.41± 0.08	1.65± 0.11	**<0.0001**	**0.0018**	**<0.0001**
Liver RAGE AU/GAPDH	0.83± 0.36	5.73± 0.41	3.63± 0.62	**<0.0001**	**0. 0227**	**0.0036**
Liver esRAGE AU/GAPDH	0.97±0.05	0.87±0.04	1.2±0.27	0.899	0.358	0.598
Liver CML AU/GAPDH	1.33±0.16	4.21± 0.59	2.56± 0.35	**0.0008**	**0.034**	0.121
Liver HMGB1 AU/GAPDH	0.21± 0.06	0.92±0.2	0.27± 0.1	**0.008**	**0.013**	0.945
Liver BAX AU/GAPDH	0.06±0.004	1.59± 0.13	0.97±0.18	**<0.0001**	**0.013**	**0.0007**
Liver Bcl AU/GAPDH	1.24± 0.3	0.13± 0.01	0.17± 0.01	**0.002**	0.985	**0.003**
Liver ADAM-10 activity AU/GAPDH	1.05± 0.12	0.28± 0.07	0.76± 0.15	**0.0016**	**0.032**	0.246
Latent MMP-9 AU/GAPDH	0.82±0.07	0.46±0.06	0.5± 0.1	**0.018**	0.921	**0.036**
Liver TIMP-1 AU/GAPDH	1.2± 0.14	2.22± 0.2	1.06± 0.13	**0.002**	**0.0007**	0.816
Liver Tyrosine hydroxylase activity (active/inactive ratio)	0.59±0.15	1.02± 0.07	0.58± 0.08	**0.032**	**0.031**	0.99
Liver norepinephrine pg/ml	31±3.2	67.1± 9.4	37.2±3.8	**0.0018**	**0.0071**	0.713
Liver ß1-AR AU/GAPDH	0.58±0.05	0.76±0.08	0.69±0.03	0.09	0.35	0.26
Liver ß2-AR AU/GAPDH	1.57±0.06	0.81±0.11	0.99±0.04	**0.001**	0.08	**0.001**
Liver ß3-AR AU/GAPDH	0.59±0.1	0.23±0.01	0.23±0.02	**0.0018**	0.99	**0.0013**

AU: Arbitrary Units; sRAGE: soluble Receptor for Advanced Glycation End products; esRAGE: endogenous secretory Receptor for Advanced Glycation End products; CML: Carboxy-Methyl-Lysine; HMGB1: High Mobility Group Box1 protein
GAPDH: Glyceraldehyde 3-Phosphate Dehydrogenase; ADRP: Adipose-Differentiation-Related-Protein
MMP: Matrix Metalloproteinase; SHRob: Spontaneously Hypertensive Obese Rat; SHRobRDN: Spontaneously Hypertensive Obese Rat with renal denervation

Table 3: Baseline characteristics of patients responding to RDN and 6 months follow-up data

	Baseline	6 months follow-up	p-value
Demographics, n=20			
Age,y	65.1±2.0	--	--
Male gender (%)	16 (80)	--	--
Body mass index, kg/m2	30.5±1.2	--	--
Risk factors			
Type II diabetes mellitus	8 (40)	--	--
Coronary artery disease	7 (35)	--	--
Cystatin C GFR, ml/min	78.5±4.8	--	--
OSAS	3 (15)	--	--
COPD	2 (10)	--	--
Stroke/TIA	1 (5)	--	--
Follow-up			
SBP, mmHg	157.4±2.6	136.5±2.5	**<0.0001**
DBP, mmHg	84.2±2.0	74.8±1.9	**<0.0001**
Office heart rate, bpm	66±3	62±2	**0.03**
ALT U/l	34.6±3.9	29.5±3.4	**0.0009**
AST U/L	29±2.3	28.2±1.8	0.52
GGT U/l	49.6±7.6	40.0±4.1	**0.04**
CHE kU/l	9.0±0.4	8.9±0.4	0.64
AP U/l	71.9±4.2	68.8±4.5	0.47
Albumine g/l	45.9±0.9	44.3±0.8	0.09
HDL mg/dl	51.1±2.7	49.3±2.8	0.22
LDL mg/dl	124.2±8.3	115±9.2	0.23
Cholesterol mg/dl	199.4±10.1	179±12.5	0.1
Triglycerides mg/dl	158.3±14	146±11	0.28
Medication			
Number of antihypertensive drugs	5±0.2	--	--
ACEi/ARB	9 (45)/15 (75)	--	--
Beta-blockers	20 (100)	--	--
Diuretics	20 (100)	--	--
Aldosterone antagonists	4 (20)	--	--
Calcium channel blockers	20 (100)	--	--
Central sympatholytics	16 (80)	--	--
Alpha-blockers	5 (25)	--	--
Aliskiren	5 (25)	--	--
Vasodilators	6 (30)	--	--
Statin	15 (75)	--	--

Categorical data are shown as number (n) and percentage of patients (%). Continuous data are expressed as mean with SEM and compared by a paired t-test. RDN: Renal Denervation; GFR: Glomerular Filtration Rate; BMI: Body Mass Index; OSAS: Obstructive Sleep Apnoe Syndrome; COPD: Chronic Obstructive Pulmonary Disease; TIA: Transient Ischemic Attack; SBB: Systolic Blood Pressure; DBP: Diastolic Blood Pressure; bpm: beats per minute; ALT: Alanine Aminotransferase; AST: Aspartate Transaminase; GGT: Gamma-Glutamyl Transferase; ACEi: Angiotensin Converting Enzyme inhibitors; ARB: Angiotensin Receptor Blocker. Bold values indicate statistically significant ($p<0.05$).

Figure 1

A

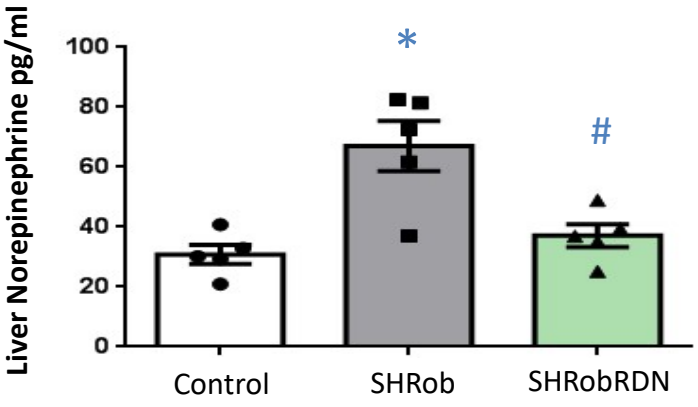

B

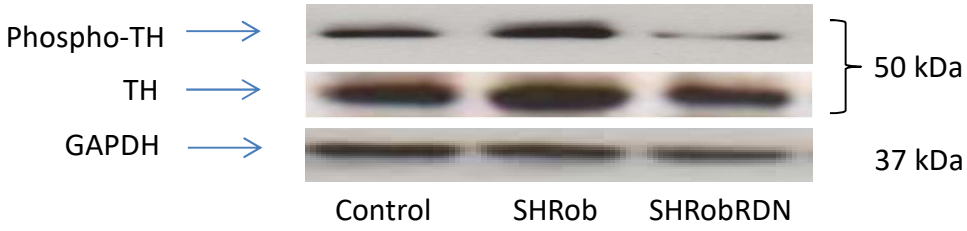

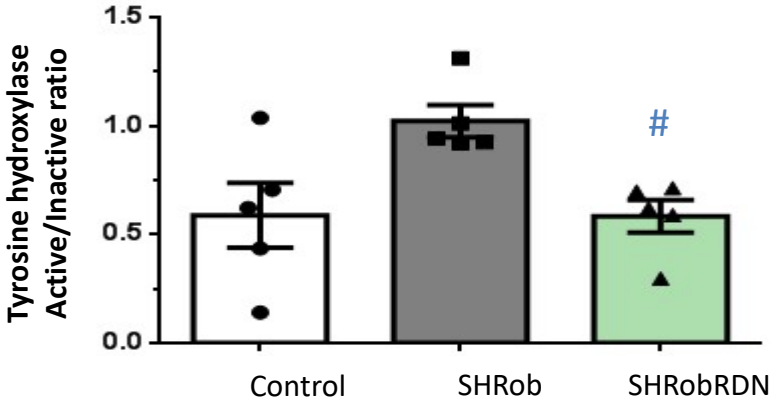

C

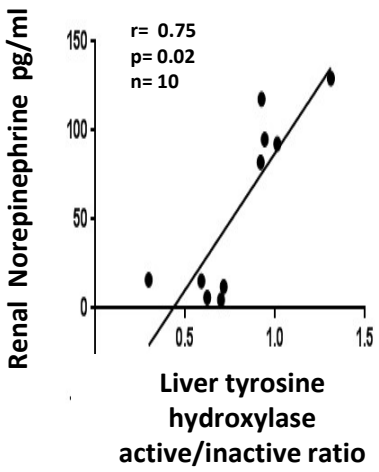

D

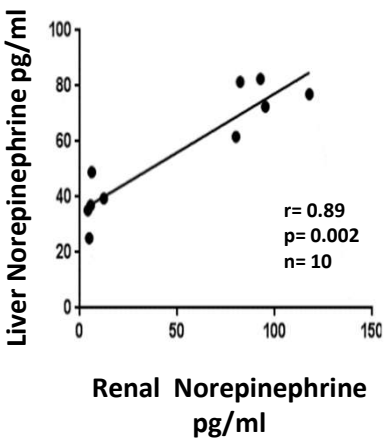

E

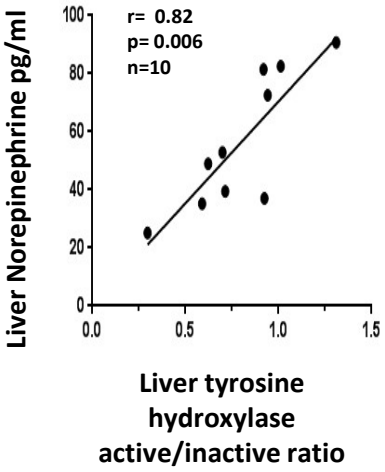

Figure 1 (continued)

F

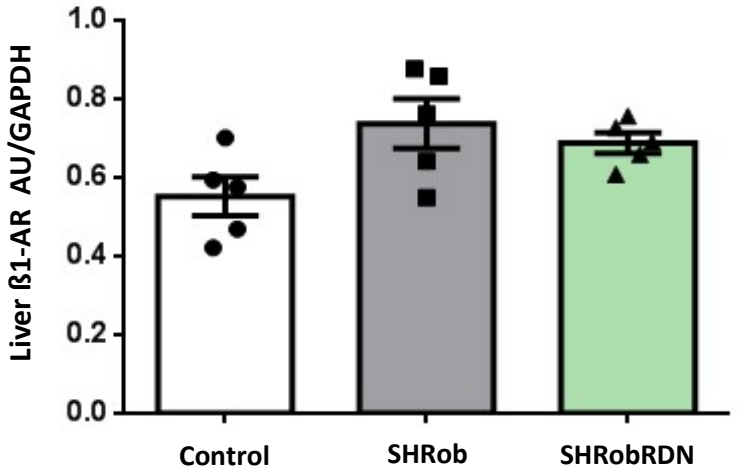

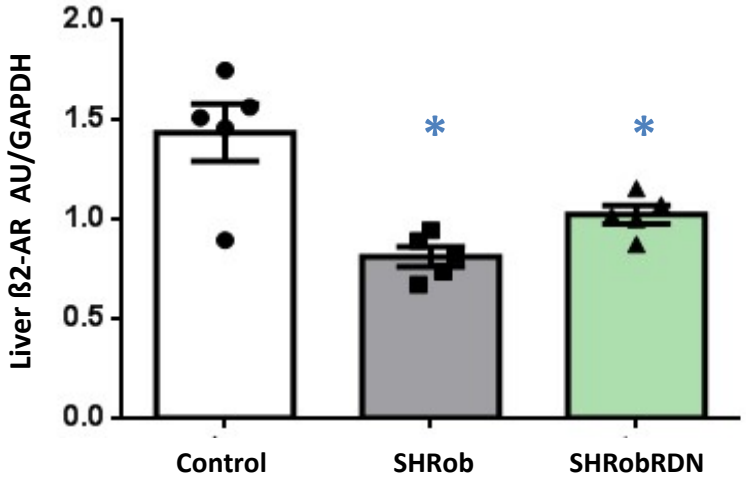

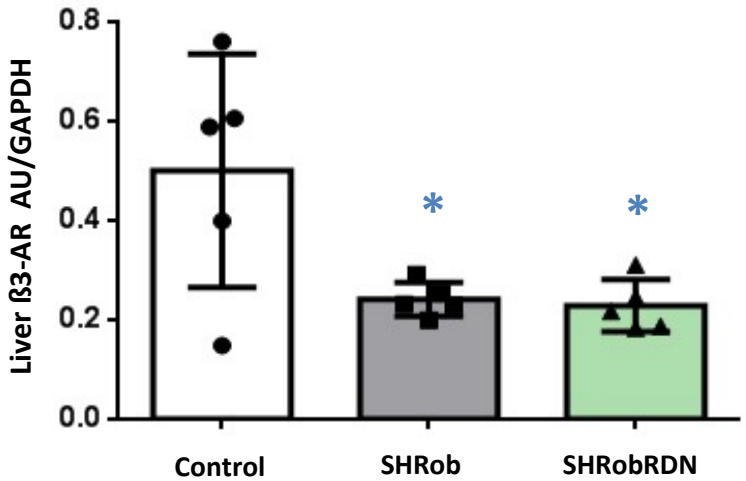

Figure 2

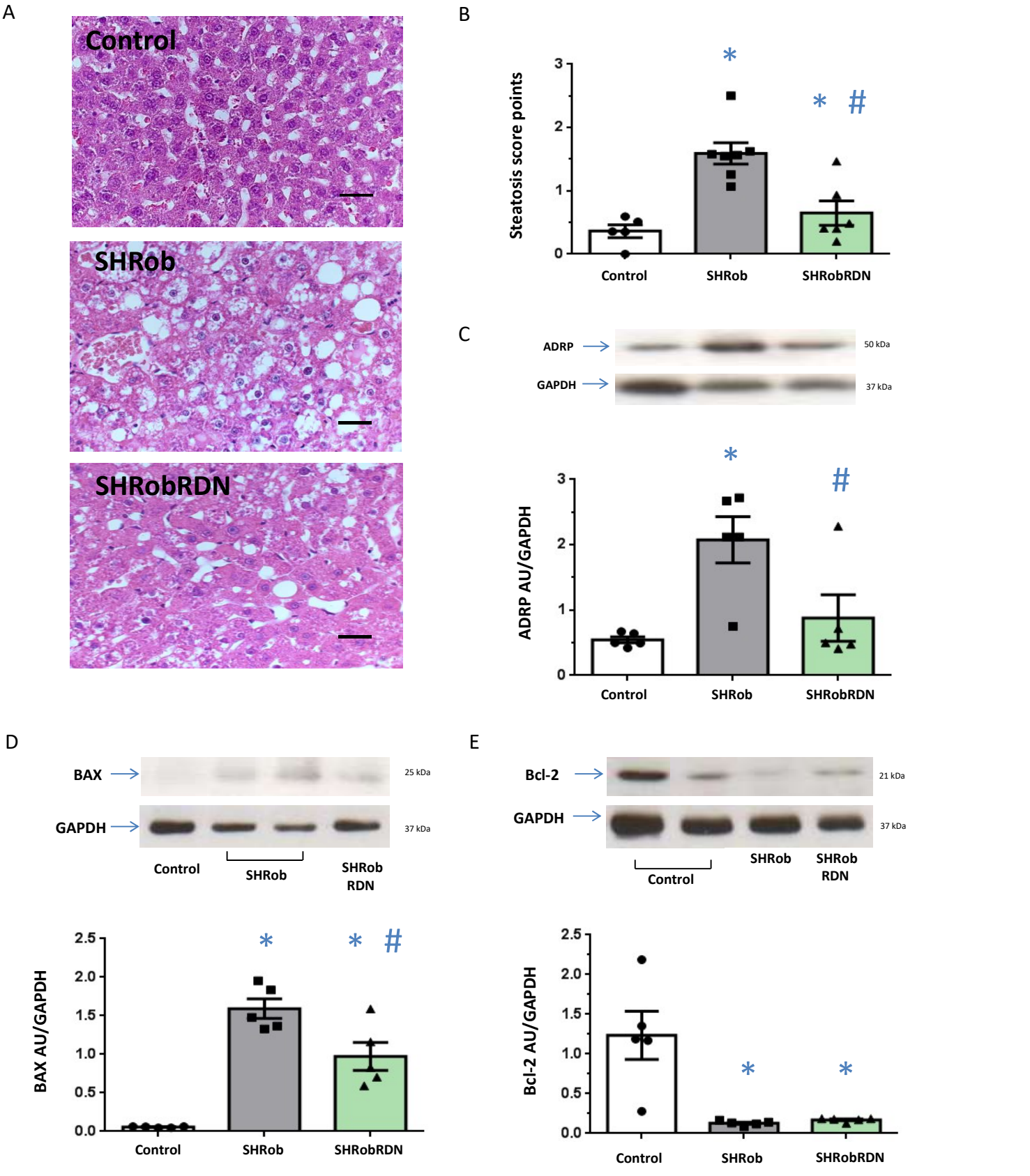
A
Control
SHRob
SHRobRDN
B
Steatosis score points
Control
SHRob
SHRobRDN
C
ADRP
GAPDH
50 kDa
37 kDa
ADRP AU/GAPDH
D
BAX
GAPDH
25 kDa
37 kDa
Control
SHRob
SHRob RDN
BAX AU/GAPDH
E
Bcl-2
GAPDH
21 kDa
37 kDa
Control
SHRob
SHRob RDN
Bcl-2 AU/GAPDH

Figure 2 (continued)

F

G

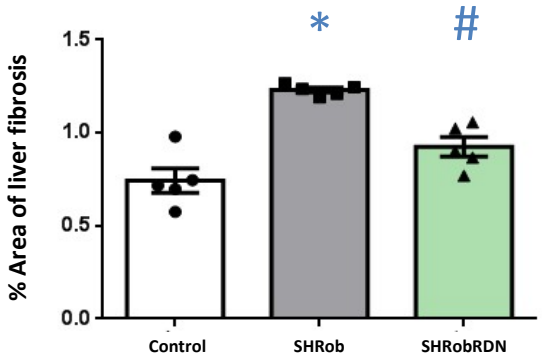

H

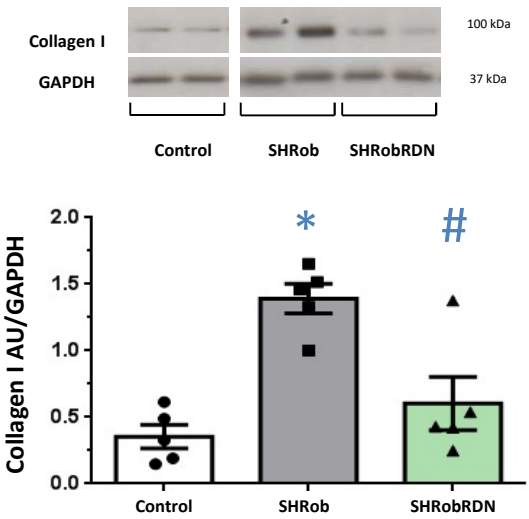

I

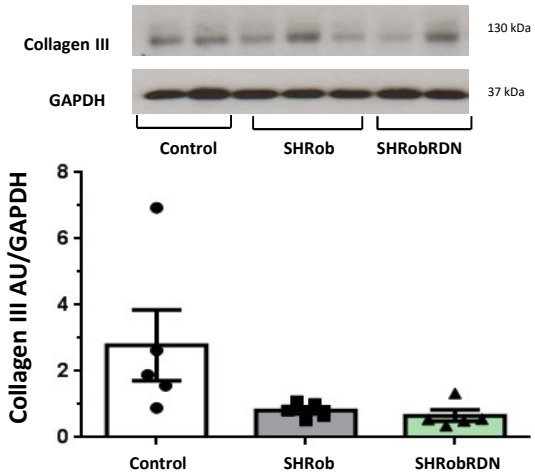

Figure 3

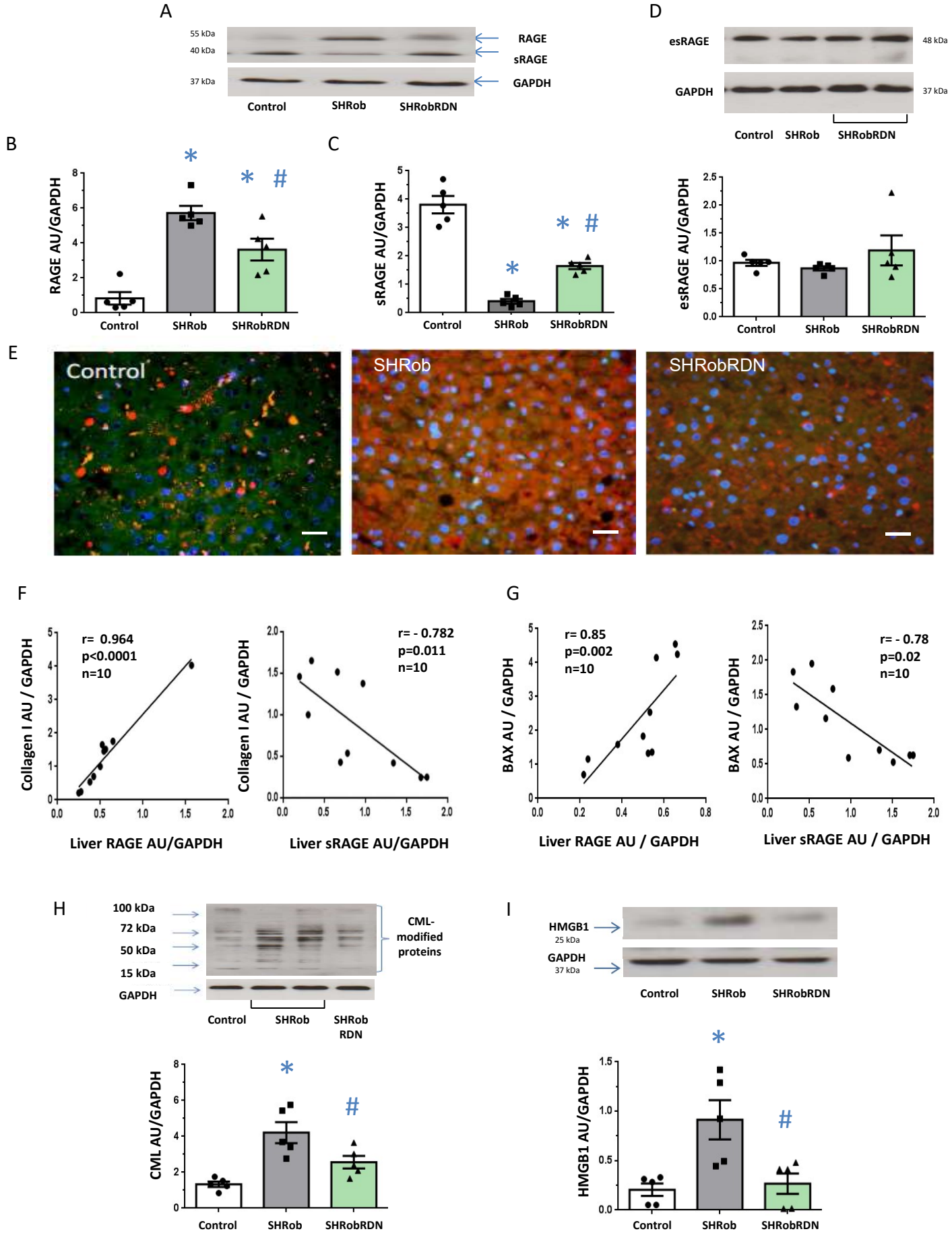
A
55 kDa
40 kDa
37 kDa
RAGE
sRAGE
GAPDH
Control
SHRob
SHRobRDN
D
esRAGE
48 kDa
GAPDH
37 kDa
Control
SHRob
SHRobRDN
B
RAGE AU/GAPDH
Control
SHRob
SHRobRDN
C
sRAGE AU/GAPDH
Control
SHRob
SHRobRDN
esRAGE AU/GAPDH
Control
SHRob
SHRobRDN
E
Control
SHRob
SHRobRDN
F
r= 0.964
p<0.0001
n=10
Collagen I AU / GAPDH
Liver RAGE AU/GAPDH
r= - 0.782
p=0.011
n=10
Collagen I AU / GAPDH
Liver sRAGE AU/GAPDH
G
r= 0.85
p=0.002
n=10
BAX AU / GAPDH
Liver RAGE AU / GAPDH
r= - 0.78
p=0.02
n=10
BAX AU / GAPDH
Liver sRAGE AU / GAPDH
H
100 kDa
72 kDa
50 kDa
15 kDa
GAPDH
CML-modified proteins
Control
SHRob
SHRob RDN
CML AU/GAPDH
Control
SHRob
SHRobRDN
I
HMGB1
25 kDa
GAPDH
37 kDa
Control
SHRob
SHRobRDN
HMGB1 AU/GAPDH
Control
SHRob
SHRobRDN

Figure 3 (continued)

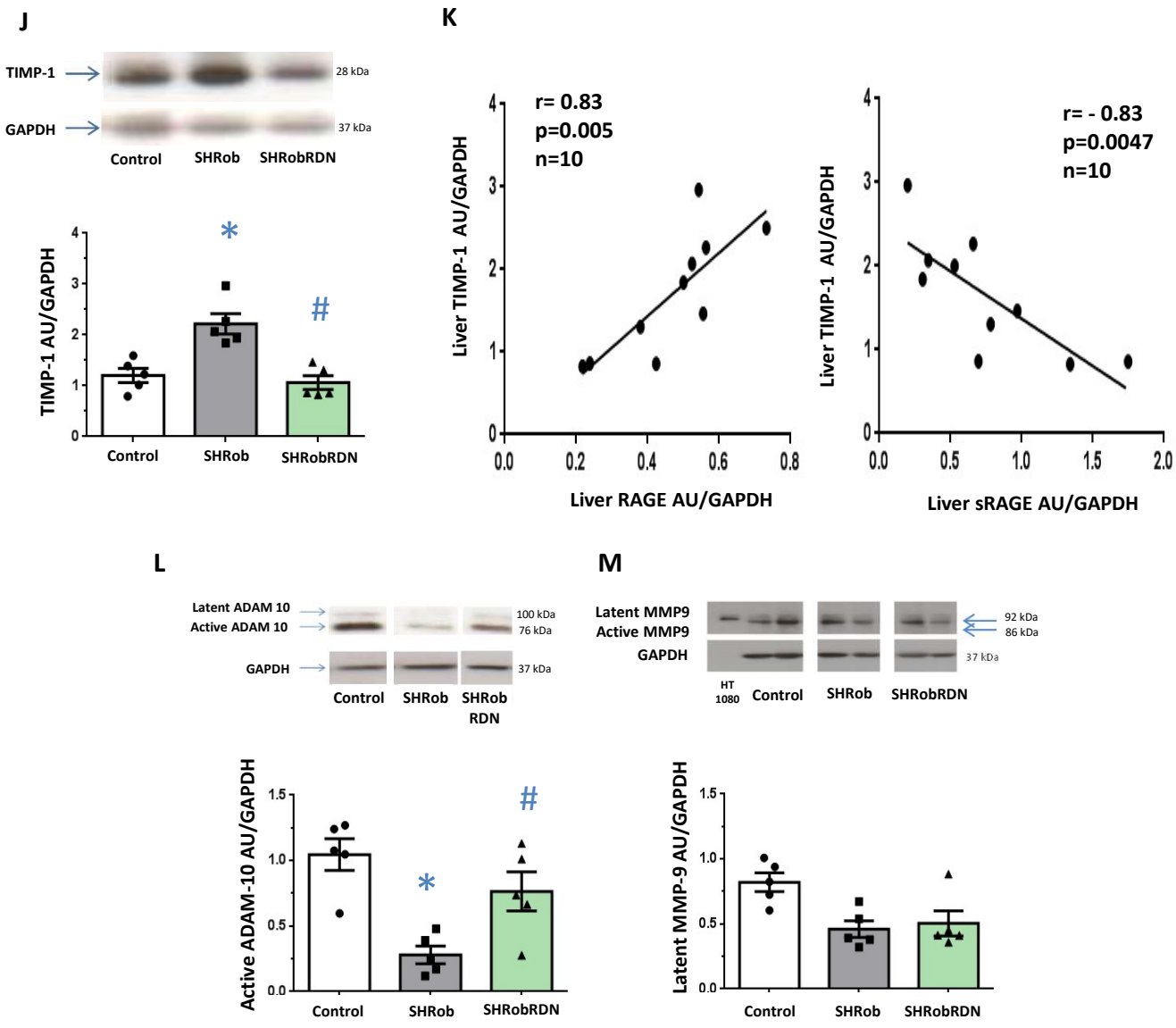

Figure 4

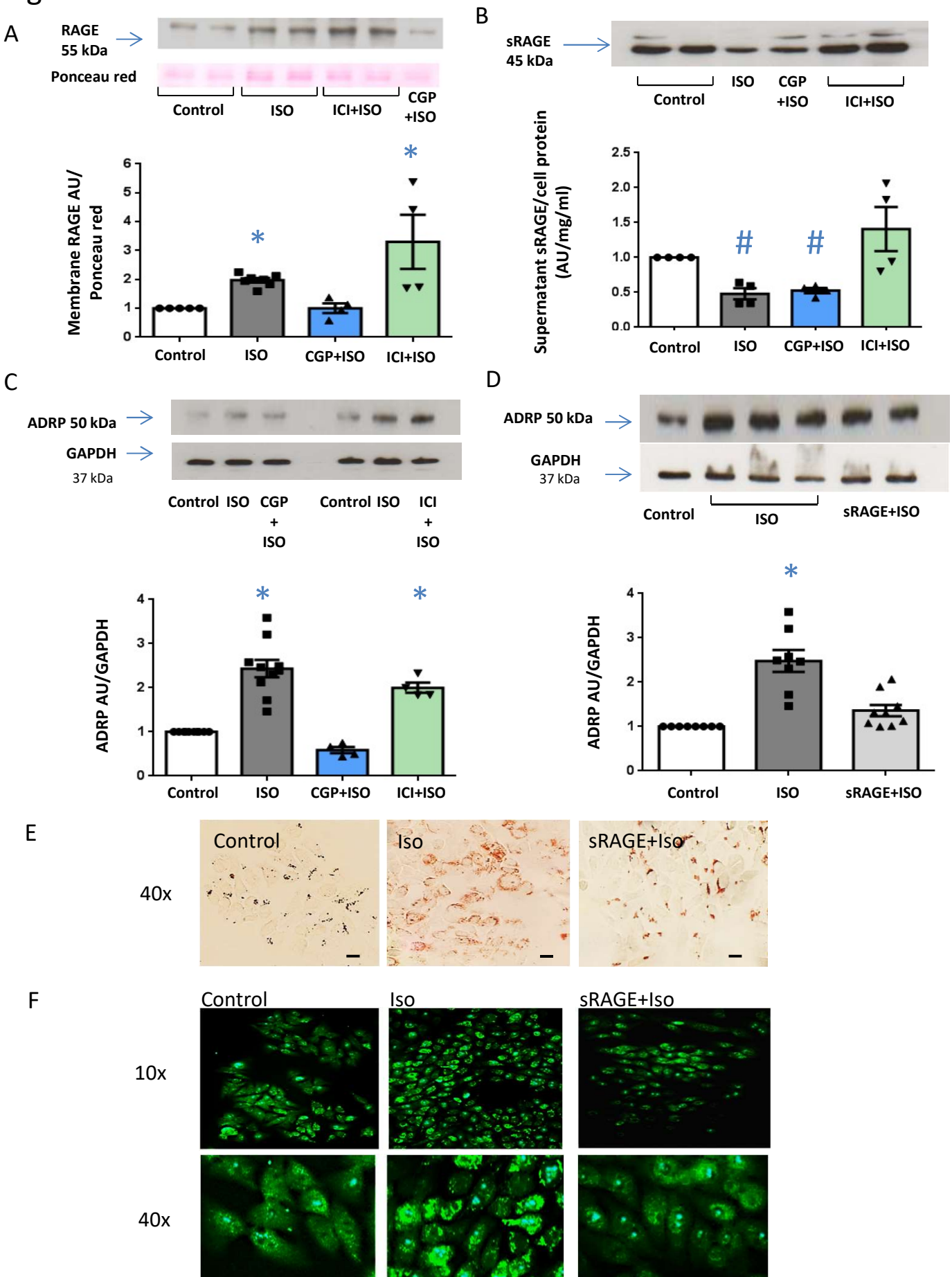
A
RAGE
55 kDa
Ponceau red
Control
ISO
ICI+ISO
CGP
+ISO
Membrane RAGE AU/
Ponceau red
Control
ISO
CGP+ISO
ICI+ISO
B
sRAGE
45 kDa
Control
ISO
CGP
+ISO
ICI+ISO
Supernatant sRAGE/cell protein
(AU/mg/ml)
Control
ISO
CGP+ISO
ICI+ISO
C
ADRP 50 kDa
GAPDH
37 kDa
Control ISO CGP + ISO
Control ISO ICI + ISO
ADRP AU/GAPDH
Control
ISO
CGP+ISO
ICI+ISO
D
ADRP 50 kDa
GAPDH
37 kDa
Control
ISO
sRAGE+ISO
ADRP AU/GAPDH
Control
ISO
sRAGE+ISO
E
40x
Control
Iso
sRAGE+Iso
F
Control
Iso
sRAGE+Iso
10x
40x

Figure 5

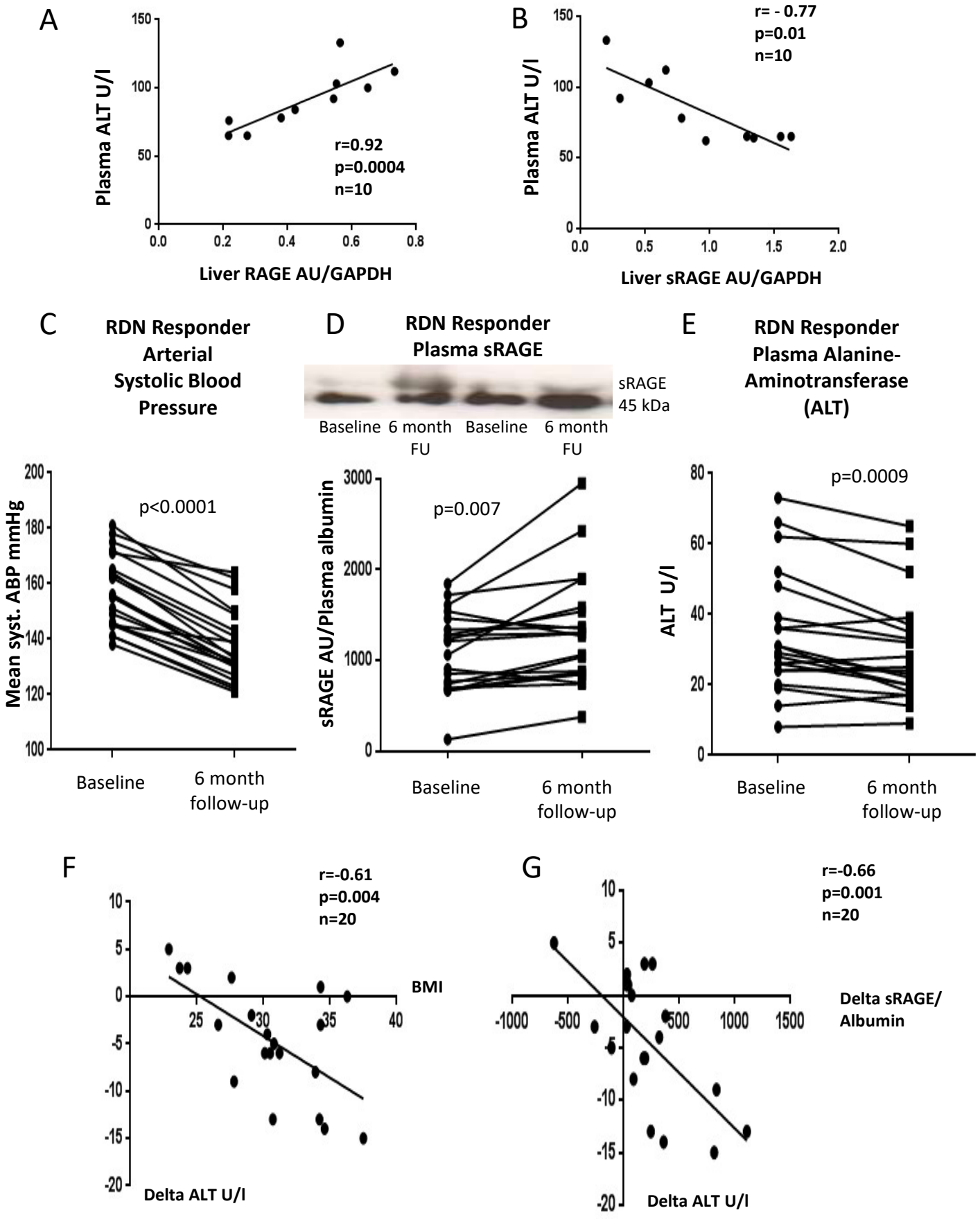
A
Plasma ALT U/l
Liver RAGE AU/GAPDH
r=0.92
p=0.0004
n=10
B
Plasma ALT U/l
Liver sRAGE AU/GAPDH
r= - 0.77
p=0.01
n=10
C
RDN Responder
Arterial
Systolic Blood
Pressure
Mean syst. ABP mmHg
p<0.0001
Baseline
6 month follow-up
D
RDN Responder
Plasma sRAGE
sRAGE
45 kDa
Baseline
6 month FU
Baseline
6 month FU
sRAGE AU/Plasma albumin
p=0.007
Baseline
6 month follow-up
E
RDN Responder
Plasma Alanine-
Aminotransferase
(ALT)
ALT U/l
p=0.0009
Baseline
6 month follow-up
F
r=-0.61
p=0.004
n=20
BMI
Delta ALT U/l
G
r=-0.66
p=0.001
n=20
Delta sRAGE/
Albumin
Delta ALT U/l

Supplement

Supplemental Figure 1

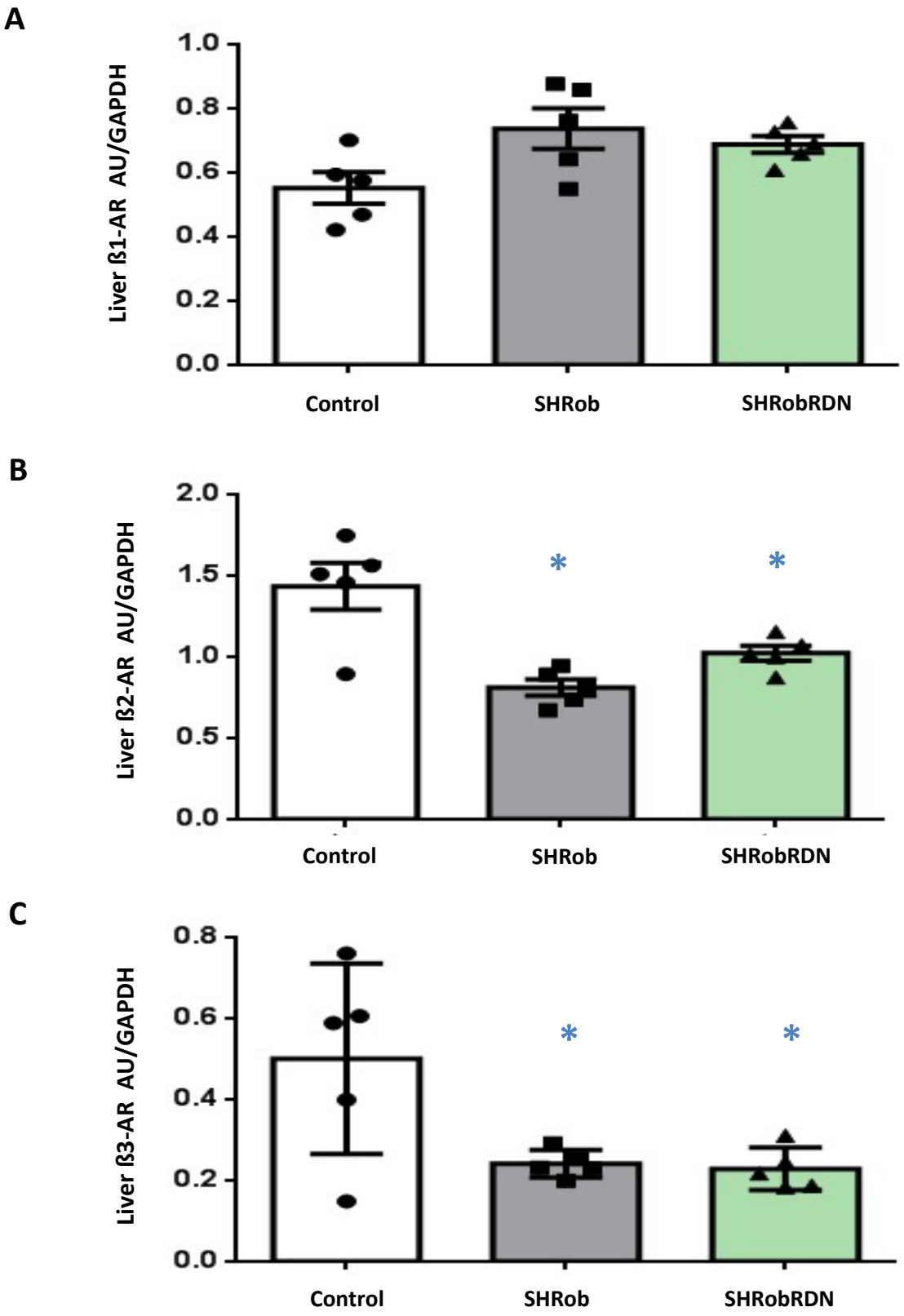

Supplemental Figure 1: A) Quantification of ß1-AR, B) ß2-AR and C) ß3-AR by Western blot in liver homogenates from normotensive lean controls (n=5), SHRob (n=5) and SHRobRDN (n=5). ß1-AR, ß2-AR and ß3-AR in arbitrary units (AU) normalized to GAPDH. *p<0.05 versus Control.

Supplemental Figure 2

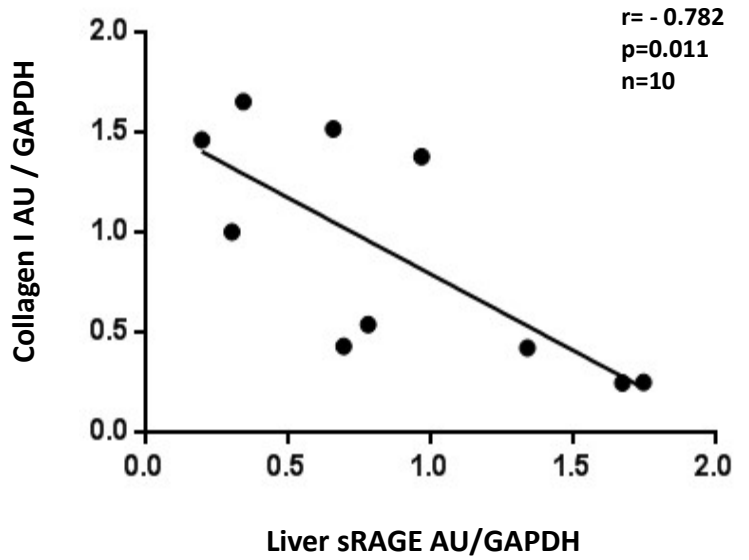

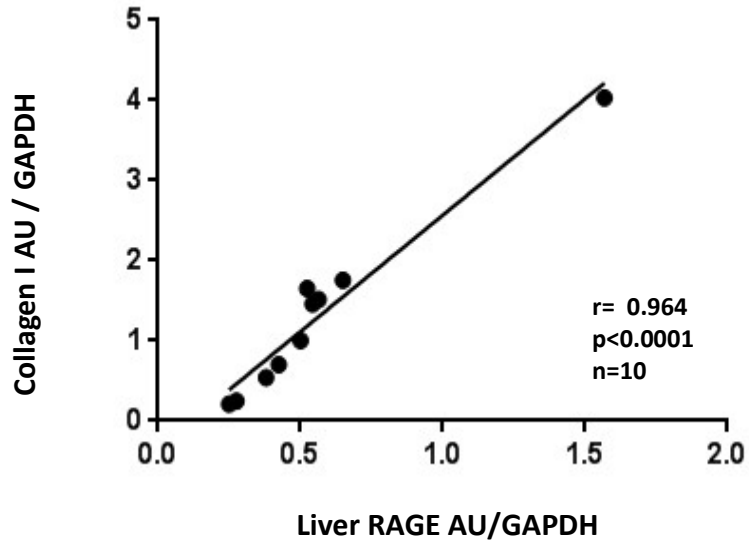

Supplemental Figure 2:
Correlation between liver sRAGE content and liver collagen I expression (upper panel) and between liver RAGE and liver collagen I expression (lower panel) in SHRob and SHRobRDN (n=10). Spearman correlation (p-value).

Supplemental Figure 3

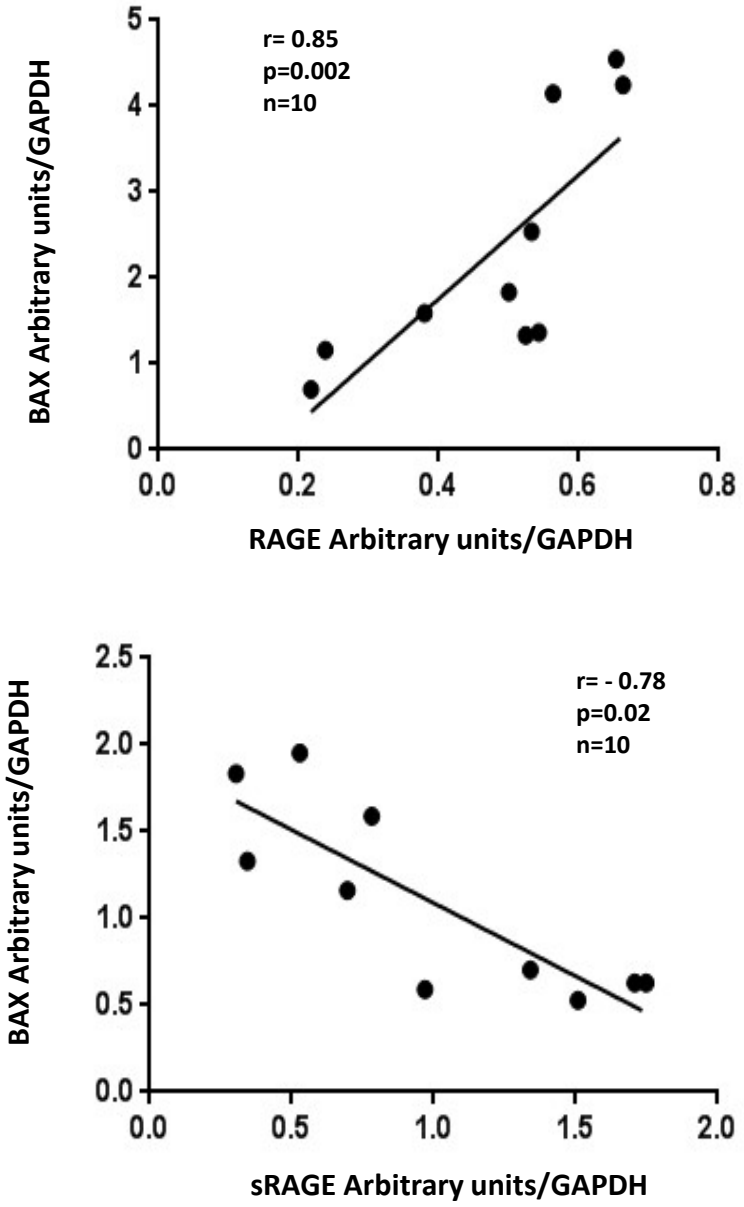

Supplemental Figure 3: Correlation between liver BAX expression and liver RAGE expression (upper panel) and between liver BAX expression and liver sRAGE expression (lower panel) in SHRob and SHRobRDN (n=10). Spearman correlation (p-value).

Supplemental Figure 4

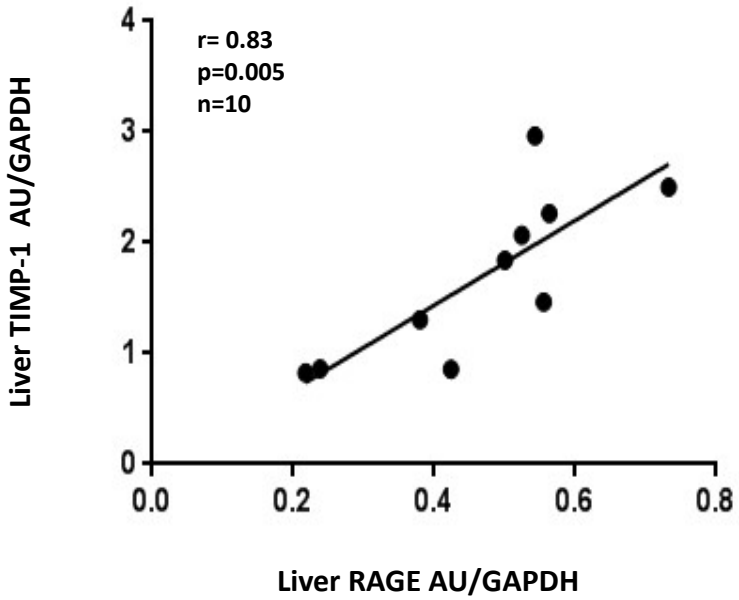

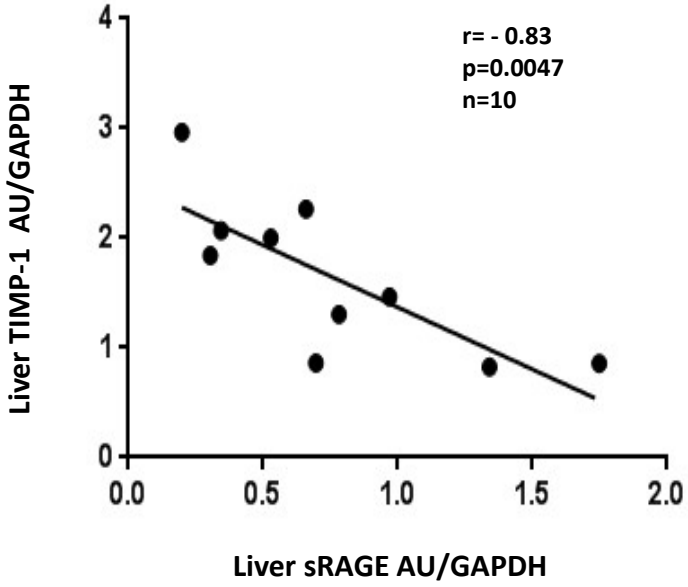

Supplemental Figure 4: Correlation between liver TIMP-1 expression and liver RAGE expression (upper panel) and between liver TIMP-1 expression and liver sRAGE expression (lower panel) in SHRob and SHRobRDN (n=10). Spearman correlation (p-value).